12-29-2023

Uncertainty Quantification of Live Load Effect in Buried RC Box Culverts

Mohd Firoj
Portland State University

Recommended Citation
Firoj, Mohd, "Uncertainty Quantification of Live Load Effect in Buried RC Box Culverts" (2023). *Dissertations and Theses.* Paper 6576.
https://doi.org/10.15760/etd.3708

Uncertainty Quantification of Live Load Effect in Buried RC Box Culverts

by

Mohd. Firoj

A thesis submitted in partial fulfillment of the
requirements for the degree of

Master of Science
in
Civil and Environmental Engineering

Thesis Committee:
David Yang, Chair
Diane Moug
Thomas Schumacher

Portland State University
2023

Abstract

Although buried and mostly invisible to the traveling public, bridge-sized culverts (i.e., culverts with span around or longer than 20 ft) account for a large proportion of state-managed bridges. As per Oregon Department of Transportation inventory, there are approximately 35,000 culverts in the state highway system. Among them, 10,862 are in poor conditions and need to be analyzed for load rating purposes. The prediction and understanding of live load effects in culverts are crucial to the design, evaluation, and life-cycle maintenance of culverts. These live load effects include maximum bending moments and shear forces at different critical cross sections.

This study focuses on the uncertainty quantification of live load effects in buried RC box culverts. The uncertainties under investigation include axle weight uncertainty within a 75-year period and model uncertainty due to the simplified load distribution model used in the current design specifications. For axle weight induced uncertainties, Monte Carlo simulation and extreme value theory are employed to calibrate live load projections, recognizing the inherent variability and uncertainty associated with long-term forecasting. To quantify the uncertainty related to the load distribution model, 680 three-dimensional finite element (FE) models of 34 culverts with 2 backfill depths (4ft and 8ft) and two types of axle load (single and tandem) are created to serve as benchmarks for different live load effects in culverts, capturing diverse geometries, material properties, and loading conditions. Concurrently, simplified two-dimensional structural frame models are established to estimate live load effects following design specifications. Live load effects obtained using both types of models are compared and analyzed in detail.

Based on the comparison, the epistemic uncertainty related to the load distribution model is quantified. The findings from this study are instrumental to the reliability-based calibration of load factors and the revision of load distribution models used for culvert design and rating.

Acknowlegments

First and foremost, I would like to express my sincere gratitude to my advisor Dr. David Yang, Department of Civil and Environmental Engineering, Portland State University for his continuous support and guidance to complete this research work. His immense knowledge, patience and faith in me have helped me to stay motivated during my entire research journey. I am also grateful for all his priceless advice on both research as well as on my career. I could not have imagined having a better advisor and mentor for my master thesis. I am especially grateful to him for going through my thesis so diligently that too making it priority over his other commitment. His painstaking efforts in editing the manuscripts of all research papers and thesis and giving useful suggestions for its improvement are gratefully and humbly acknowledged.

I would also like to thank the other members of my thesis committee, Dr. Diane Moug and Dr. Thomas Schumacher for their availability, valuable insights and suggestions. My sincere thanks are due to Dr. Peter Duskika, Head, Department of Civil and Environmental Engineering, Portland State Univeristy for extending every possible support during the work. My thanks and appreciations are due to all the technical and non-technical staffs specilally for Kiley Melicker, Sam Parsons and Sarah Phillips of the Department of Civil and Environmental Engineering for all their support.

I gratefully recognize the financial support in the form of graduate research assistantship provided by the Department of Civil Engineering at Portland State University (PSU). I cherish and treasure the friendships that have been forged during my time at PSU. A special thanks to Mr. Antenah Debornia, Mr. Sina Damavodi, Mr. Amir, Mr. Ali

Algamadi, Dr. Ashish Bahuguna and Mr. Tariq Mansoor, for making this journey so much fun and memorable, and most importantly, keeping me sane throughout the whole process. I could not have made it without you all.

Finally, I would like to deeply thank my father, Dr. Mohd Noman, mother, Smt. Meer Jahan, brother, Mr. Mohd Azam, and my wife Ms. Gulafsha for their unconditional and endless love, support and encouragement throughout. This thesis is dedicated to them. I would also like to express my indebtedness for their immense faith in me.

Table of Contents

List of Tables

List of Figures

Abbreviations

Abbreviation	Description
2D	Two dimensional
3D	Three dimensional
ADTT	Average daily truck traffic
CDFs	Cumulative distribution functions
COV	Coefficient of variance
DOFs	Degree of freedoms
FEM	Finite element method
LRFD	Load and resistance factor design
MCS	Monte Carlo Simulation
PDF	Probability density functions
RC	Reinforced concrete
SSI	Soil-structure interaction
WIM	Weigh in motion

Chapter 1

Introduction

1.1 Background

Culverts play an important role in transportation infrastructure. Among all types of culverts, Reinforced Concrete (RC) box culverts are known for their strength and ability to withstand tough environmental and traffic conditions. In certain conditions, culverts may be more economically attractive than bridge where the bridges are not hydraulically required and where debris and ice potential are tolerable (Schall, 2012). Although consequences of culvert failures might be less critical than bridges because of their smaller scales and locations beneath the road embankment, significant losses such as highway service disruption can still occur due to culvert failures (Scanlon, 2012).

The understanding of live load distribution on these culverts is important to their design, evaluation, and long-term maintenance. The quantification of live load effects in culverts and their uncertainties are faced with two major challenges:

(a) The live load effects of culverts are controlled by the axle weights of passing vehicles. This load spectrum can be drastically different from the spectrum of gross vehicle weight used to calibrate the uncertainties in conventional bridges.
(b) RC culverts are buried structures with soil backfill. This backfill complicates the load distribution from the road surface to the buried culverts. The uncertainty

related to the design load distribution models differs from the epistemic uncertainties related to the structural analysis models of conventional bridges.

To overcome these challenges, the first goal of this research is to quantify the uncertainty due to live load over the buried RC box culvert in the design service life of 75 years. To accomplish this objective, representative culverts were selected based on different geometric configurations and loading conditions. These culverts were analyzed for single-axle and tandem loading based on weigh-in-motion (WIM) data with Monte Carlo simulation (MSC). The analyses were carried out with two-dimensional (2D) frame model and LRFD live load distribution model through backfill soil (AASHTO, 2019). The second goal is to quantify the epistemic uncertainty related to live load distribution model by considering soil-culvert interaction using three-dimensional (3D) finite element (FE) analysis.

1.2 Scope of Work: Representative Culverts

Key factors influencing the safety of culverts can be categorized into three primary groups: structural factors, loading factors and analytical factors. These categories directly impact the probability of culvert failure. Herein, the objective focuses primarily on structural and loading factors as they play a pivotal role in establishing representative culvert populations.

1.2.1 Key Factors Affecting Culvert Safety: Structural Factors

Structural factors encompass various elements such as the geometric attributes of culverts, the material properties of culverts, reinforcement layout of culvert components,

and the age and condition of culverts. These structural factors dictate a culvert's load-carrying capacity and its response to external loads. For instance, the dimensions of slabs and walls in an RC box culvert can influence load distribution among different members, while reinforcement details impact flexural and shear capacities, as well as the fixity at slab-wall joints. These factors are pivotal when collecting typical culverts in the present study. In this study, the maximum live load effect in terms of bending moment and shear force is analyzed at various critical locations of culverts.

1.2.2 Key Factors Affecting Culvert Safety: Loading Factors

Loading factors include variables such as different types of heavy vehicles (e.g., design and legal loads), average daily truck traffic (ADTT) and weight spectrum, backfill/subgrade properties, and the dynamic impact of moving loads on culverts. These factors directly influence the magnitude and distribution of load effects on a culvert. Culverts exhibit unique characteristics due to (a) the attenuation of surface live load to the buried structure, (b) the effects of SSI, and (c) axle weight spectrum and multi-lane presence statistics. The attenuation of load and SSI are linked to the backfill depth, necessitating consideration of various backfill depths when collecting representative culverts. Moreover, due to the relatively short span of culverts, live loads are typically dominated by axle weight rather than gross vehicle weight, which is the conventional parameter in bridge design. The statistics of multi-lane presence may also differ significantly from those of gross vehicle weights. To study uncertainties related to the backfill load distribution, this study is focused on two backfill depth (4 ft and 8 ft), representing moderate to high backfill depths. Two dominant types of axle configurations, single and tandem axles, are considered in the structural analysis.

1.2.3 Key Factors Affecting Culvert Safety: Analytical Factors

Analytical factors pertain to decisions regarding structural analysis methods and their associated parameters. These methods vary in complexity, from planar linear models to 3D FE models incorporating full SSI effects and nonlinear behaviors. While AASHTO LRFD (2019) focuses on 2D evaluation models in line with MBE and LRFD specifications, more intricate models with enhanced simulation capabilities, such as FE models with SSI, are required for precise estimation of structural behaviors and statistical quantification of model errors in 2D evaluation models. Various finite element packages have been reviewed to facilitate this quantification effort, including CANDE, LUSAS, ABAQUS, and PLAXIS. Analytical factors, though not affecting the collection of typical culverts, are relevant to the task of uncertainty quantification.

1.2.4 Collection of Representative Culverts

Based on the key factors summarized above, Table 1.1 shows the 34 representative culverts analyzed in this study. For each culvert, two backfill depths (4 ft and 8 ft) are considered. The critical cross sections under consideration are presented in Figure 1.1. Note that only top slab is analyzed in this study. This is because the current LRFD live load distribution model does not have detailed specifications on load attenuation through the culvert depth, resulting in excessively overestimated load effects below the top slab (Wood, et al., 2016) whose uncertainties are difficult to quantify.

For two-cell culverts, the load effects under consideration are the negative bending moment and shear force at S1 (exterior wall-slab corner), positive bending moment at S2 (cell midspan), and negative bending and shear at S3 (mid wall-slab corner). For one-cell

culverts, only the load effects at S1 and S2 are considered because of the symmetry of maximum load effects in S3 and S1. The choice of using the mid-span location for positive bending moments is due to culverts are subjected to relatively uniform loading. In such situations, the maximum moment typically occurs near the center, making the mid-span location a reasonable approximation. Shear force in design is considered at a distance (effective depth) away from the section. However, the objective herein is to quantify the uncertainty in calculating the maximum shear force.

Given the number of culverts and the associated analyses at different cross sections and under different axle loads, it is impractical to analyze all representative culverts manually. Therefore, an automated procedure is developed to analyze these culverts. The 2D structural frame models were developed in OpenSeesPy ((Zhu, et al., 2018); (McKenna, 2011)), while 3D FE analyses were carried out via ABAQUS Python Script (Zuo & Xie, 2015).

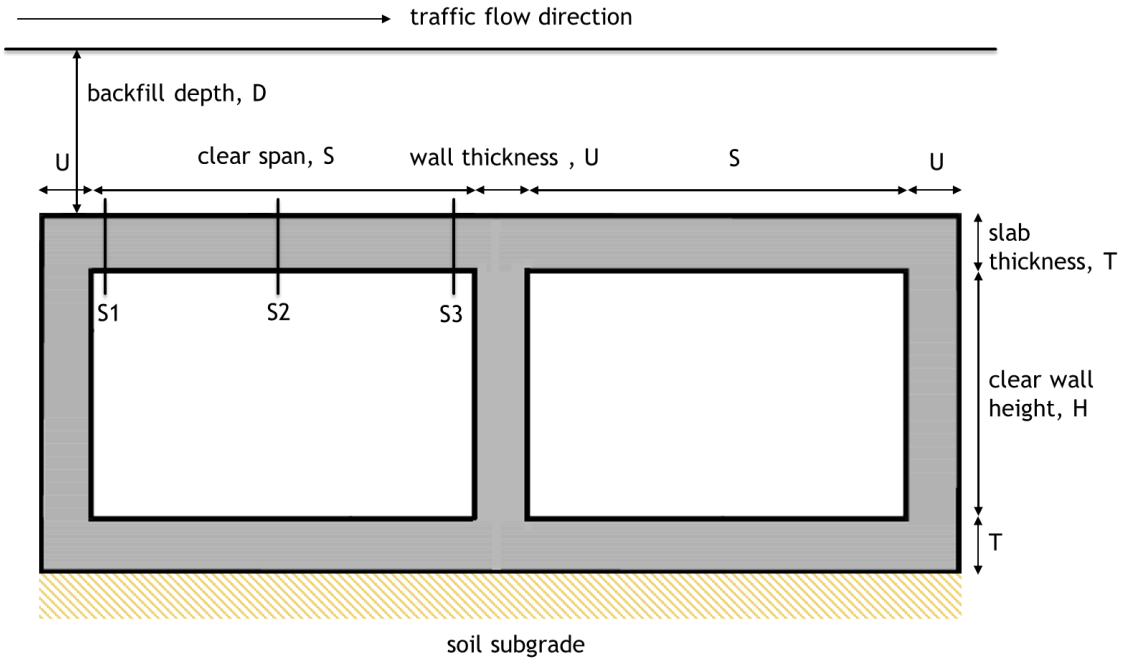

Figure 1.1: Critical locations of interest in a typical culvert

Table 1.1: Populations of culverts with varying geometry and backfill depth

Culvert ID	Number of cells	Backfill depth, D (ft)	Clear span length S (ft)	Clear wall height H (ft)	Thickness (in)	
					T slab	U wall
1	1	4,8	10	4	9	8
2	1	4,8	10	6	9	8
3	1	4,8	10	8	9	8
4	1	4,8	10	10	9	8
5	1	4,8	12	6	10	8
6	1	4,8	12	8	10	8
7	1	4,8	12	10	10	9
8	1	4,8	12	12	10	9
9	1	4,8	14	8	12	10
10	1	4,8	14	10	12	10
11	1	4,8	14	12	12	12
12	1	4,8	14	14	12	12

13	1	4,8	16	6	12	10
14	1	4,8	16	8	12	10
15	1	4,8	16	10	12	12
16	1	4,8	16	12	12	12
17	1	4,8	24	8	16	12
18	2	4,8	6	2	8	6
19	2	4,8	6	4	8	6
20	2	4,8	6	6	8	6
21	2	4,8	8	4	9	6
22	2	4,8	8	6	9	7
23	2	4,8	8	8	9	7
24	2	4,8	10	4	9	8
25	2	4,8	10	6	9	8
26	2	4,8	10	8	9	8
27	2	4,8	10	10	9	8
28	2	4,8	12	6	10	8
29	2	4,8	12	8	10	9
30	2	4,8	12	10	10	10
31	2	4,8	12	12	10	10
32	2	4,8	14	8	12	10
33	2	4,8	14	10	12	10
34	2	4,8	14	12	12	12

Chapter 2

Literature Review

2.1 Background: Design Specifications for Live Loads on Culverts

Figure 2.1 shows the variations of the live load distribution over the buried box culvert using the AASHTO LRFD specifications (2019). The equation used in the current LRFD for the live load distribution over the backfill was last modified based on the finite element analyses of RC box culvert as reported in NCHRP Report 647 (Petersen, et al., 2010).

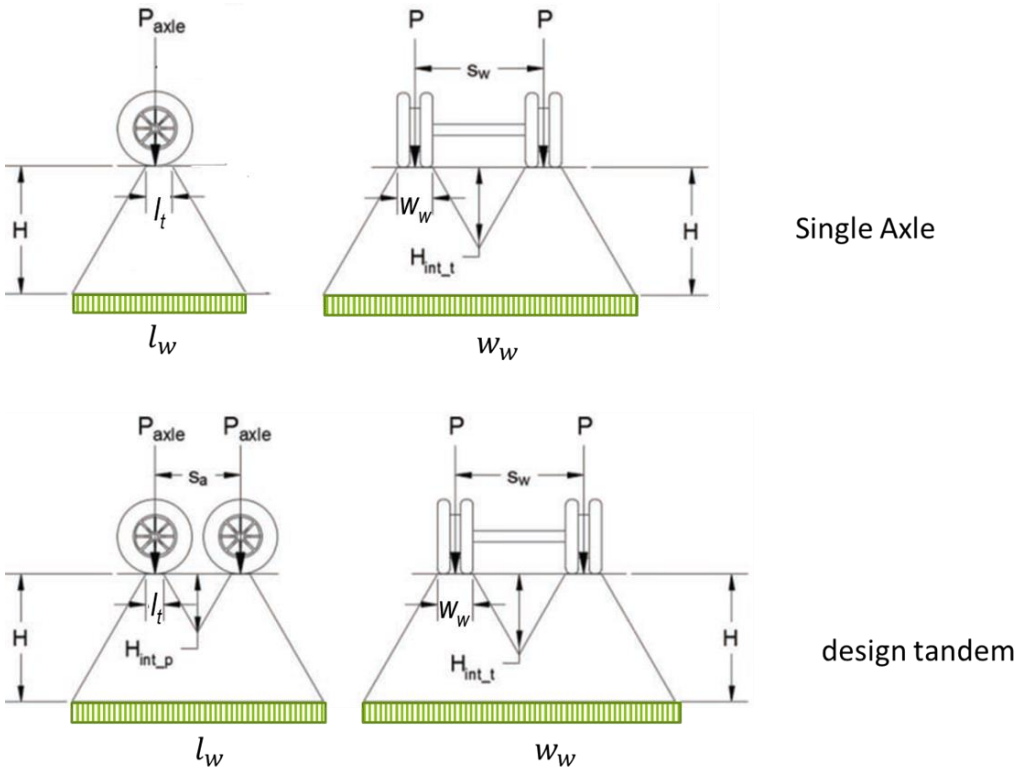

Figure 2.1: Live load variations with the backfill depth for buried RC box culvert

For comparison purposes, the interaction wheel depth and area of live load distribution in both current (AASHTO, 2019) and the previous standard specifications (AASHTO, 2002) is listed in the Table 2.1

Table 2.1: Comparison of live load distribution as per current AASHTO LRFD (2019) and AASHTO standard (2002)

AASHTO LRFD (2019)	**AASHTO LRFD (2002)**
$H_{int-t} = \frac{s_w - \frac{w_t}{12} - \frac{0.06D_i}{12}}{LLDF}$	$H_{int-t} = \frac{s_w}{LLDF}$
$H_{int-p} = \frac{s_a - \frac{l_t}{12}}{LLDF}$	$H_{int-p} = \frac{s_a}{LLDF}$
$H_{int-s} = \frac{s_s - \frac{w_t}{12} - \frac{0.06D_i}{12}}{LLDF}$	$H_{int-s} = \frac{s_s}{LLDF}$
$A_{LL} = w_w l_w$	$A_{LL} = w_w l_w$
$P_L = \frac{P\left(1 + \frac{IM}{100}\right)m}{A_{LL}}$	$P_L = \frac{P\left(1 + \frac{IM}{100}\right)m}{A_{LL}}$
$w_w = LLDF(H) + \frac{w_t}{12} + \frac{0.06D_i}{12}$ if $H < H_{int-t}$	$w_w = LLDF(H)$ if $H < H_{int-t}$
$w_w = LLDF(H) + \frac{w_t}{12} + \frac{0.06D_i}{12} + s_w$ if $H \geq H_{int-t}$	$w_w = LLDF(H) + s_w$ if $H \geq H_{int-t}$
$l_w = LLDF(H) + \frac{l_t}{12}$ if $H < H_{int-p}$	$l_w = LLDF(H)$ if $H < H_{int-p}$
$l_w = LLDF(H) + \frac{l_t}{12} + s_a$ if $H \geq H_{int-p}$	$l_w = LLDF(H) + s_a$ if $H \geq H_{int-p}$

Where, A_{LL} Rectangular area at depth H (ft.^{2})

Di Inside diameter or clear span of culvert (in.)

$H_{int\text{-}p}$ Axle interaction depth parallel to culvert span (ft.)

$H_{int\text{-}s}$ Adjacent trucks interaction depth transverse to culvert span (ft.)

$H_{int\text{-}t}$ Wheel interaction depth transverse to culvert span (ft.)

IM Impact factor (%)

$LLDF$ Live load distribution factor

l_t Tire patch length, 10 (in.)

l_w Live load patch length at depth H (ft.)

m Multiple presence factor

P Live load applied at surface of all interacting wheels (kip)

P_L Live load vertical stress at depth H (ksf)

s_a Axle spacing, 14 for HL-93 design truck, 4 for HL-93 design tandem (ft.) Axle spacing, 14 for HS-20 truck (ft.)

s_s Minimum spacing between trucks, 4.0 (ft.)

s_w Wheel spacing, 6.0 (ft.)

w_t Tire patch width, 20 (in.)

w_w Live load patch width at depth H (ft.)

2.2 Past Studies

In 1994, AASHTO introduced the Load and Resistance Factor Design (LRFD) methodology to enhance safety standards in bridge design, marking a significant shift from the previous Standard Specifications for highway bridges (McGrath, et al., 2005). The objective was to establish a code based on reliability principles, aiming to deliver a consistent level of safety that surpassed the previous Standard Specification for Highway Bridges (Rund & McGrath, 2000).

The effect of live load depends on many parameters including the span length, truck weight, axle loads, axle configuration, position of the vehicle on the bridge (Nowak, 1999). For short-span bridges and culverts, the weight of the individual axle or axle group can be more important than the gross vehicle weight (GVW), and these need to be represented accurately in simulations (O'Brien, et al., 2005). In this context, (Lawson, et al., 2018) find out that axle loads associated with the HS-20 standard truck compared to the gross vehicle weight tend to control the load rating for most culvert applications.

Over the years, several significant studies have been carried out to understand the live load distribution in RC box culverts. Based on field studies and numerical analyses, 2D structural frame model with LRFD live load distribution model can overly estimate the load demand in culverts ((Katona, 2019); (Sharifi, et al., 2023)). For instance, (Orton, et al., 2015) carried out the field testing of the 2-cell culvert and found that the strain near maximum positive moment and the vertical displacement right beneath the live load are overestimated when using 2D frame model and LRFD live load distribution model. (Acharya, et al., 2016) conducted a numerical analysis of low backfill box culverts (backfill smaller than 2ft) using the finite difference method, and compared vertical pressure thus obtained with that estimated with the LRFD distribution model. The results also demonstrated that the LRFD distribution model overestimates pressure on culverts, especially for low-fill culverts under rigid pavement. This observation aligns with the concern raised by (TRB Committee AKB70, 2013) (formerly AFF70) about excessively conservative load distribution models leading to unrealistically low rating factors. This challenge of balancing conservatism in design and load rating is further emphasized and

investigated by other studies ((NCHRP, 2015); (Lawson, et al., 2010); (Han, et al., 2009) and (Orton, et al., 2015)).

2.3 Research Gaps

From the previous literature review, there exist significant research gaps that deserves further investigation. These research gaps are summarized as follows:

1. Due to the relatively short span, the safety of a culvert is controlled by the axle weight instead of the gross vehicle weight. As a result, the uncertainty characteristics due to random vehicle passages can be different from those in bridges.
2. Limited emphasis on 3D finite element modeling: Previous research predominantly relies on simplified 2D structural frame models to analyze RC box culverts. This simplification cannot fully capture the complex interaction between the culvert and surrounding soil.
3. Limited probabilistic analysis: Prior research focuses primarily on the deterministic analysis of live load distribution, with an aim to develop more accurate distribution models. There lacks a systematic probabilistic analysis in bending moments and shear forces at different cross sections obtained from these models.

In summary, the identified research gaps emphasize the need for more advanced modeling techniques and systematic uncertainty quantification in order to enhance the

understanding and engineering practices related to the design and evaluation of RC box culverts.

2.4 Objectives of Research

To address the research gaps, the present study has the following objectives:

1. Develop the methodology for the uncertainty quantification of live load effect over the buried RC box culvert under the axle weight spectrum.
2. Quantify the uncertainty in live load effects in buried RC culverts using Monte Carlo simulation.
3. Develop and validate 3D FE models of RC box culverts that accounts for 3D load distribution through soil-culvert interaction.
4. Automate the process for 2D and 3D culvert analyses, allowing efficient investigation for all representative culverts and load effects.
5. Conduct a comparative analysis of live load distributions between the 3D finite element model and a 2D structural frame model, focusing on critical locations of the culverts and assessing demand parameters, including bending moments and shear forces, to better understand structural behavior under different loading conditions.

Chapter 3

Uncertainty Quantification of Culvert Live Load Effects

The live load effect at the critical locations can be determined using the structural frame model and finite element model as discussed in Chapter 4 and Chapter 5, respectively. To identify the critical location causing the maximum load effect, the axle load is moved along the traffic direction, and the load effects are estimated using the 2D frame analysis and LRFD distribution model. The locations resulting in the maximum load effect for all targeted load scenarios (single axle and tandem) are recorded and used as input in 3D FE analysis.

The maximum live load effect under consideration, L_{max}, can be modeled as the product of three random variables, expressed as follows

$$L_{max} = \lambda_{LDS}.L_{frame}.\lambda_{IM} \tag{3.1}$$

where, λ_{LDS} = ratio live load effect from FEM analysis to the structural frame model analysis; L_{frame} = live load effect obtained using 2D frame analysis and LRFD distribution model. IM = dynamic impact ($IM \geq 1$). Using equation (3.1) and assuming the statistical independency of the three random variables, the mean and coefficient of variance (COV) of the live load effect can be approximated as follows:

$$\bar{L}_{max} = \bar{\lambda}_{LDS}.\bar{L}_{frame}.\bar{\lambda}_{IM} \tag{3.2}$$

$$V_{L,max}^2 = V_{\lambda,LDS}^2 + V_{L,frame}^2 + V_{IM}^2 \tag{3.3}$$

The uncertainty quantification due to random vehicle passage can be obtained with Monte Carlo Simulation (MCS) based on the axle load spectrum processed from axle weigh in motion (WIM) data as reported in NCHRP report 683 (Sivakumar, et al., 2011). To generate samples of load effects under uncertain axle weights and configuration, the linear elasticity of the 2D frame model is leveraged. Specifically, the load effects are first computed for (a) a unit load of 1 kip distributed over two tire contact areas and (b) two-unit loads, spaced 4 feet apart, distributed over four tire contact areas. Both load patterns are distributed through the backfill based on LRFD distribution model. The resulting load effects are then multiplied with the samples of axle weights and configurations to obtain samples of load effects. Based on these samples, $\bar{L}_{frame}$ and $V_{L,frame}$ can be calculated.

Based on (Sivakumar, et al., 2011), site and data variation related to the WIM records can result in additional uncertainty in the live load effect L_{frame}. Herein, this additional variation is added to $V_{L,frame}$ based on the following equation:

$$V_{L,frame}^2 = V_{axle}^2 + V_{site,data}^2 \tag{3.4}$$

where V_{axle} = COV from MCS samples, obtained using the procedure previously described; $V_{site,data}^2 = 0.045^2 + 0.02^2$ by assuming COV of 0.045 for site statistic and COV of 0.02 for data statistic (Sivakumar, et al., 2011).

The factor λ_{LDS} is calibrated based on the structural frame and 3D finite element model response (negative and positive bending moment, shear force) as discussed in Chapter 5. This factor is defined as the ratio of response using the finite element model to that of structural frame model. The mean ($\bar{\lambda}_{LDS}$) and COV ($V_{\lambda,LDS}$) of the factor (λ_{LDS}) can be

determined with statistical analysis. However, in the present study, the focus is solely on calculating the factor λ_{LDS}.

Due to the backfill depth, dynamic effect for a culvert is different from that for a girder bridge (Kadivar, et al., 2018). In particular, the soil layer functions as a damper that reduces the load amplification on the culvert. In LRFD, this decrease in dynamic effect is reflected by reducing the nominal IM from 1.33 to the following equation which depends on the backfill depth (D)

$$IM = 1.33 \times \left(1.0 - \frac{D}{8}\right) \geq 1 \tag{3.5}$$

The bias factor associated with Equation (3.5) is assumed to be one due the lack of reliability data (i.e., no bias), namely, the mean value ($\overline{IM}$) of dynamic effect is the same as its nominal value. Hence, the mean value of dynamic effect ($\overline{IM}$) can be calculated as follows:

$$\bar{\lambda}_{IM} = 1 + IM \tag{3.6}$$

According to (Nowak, 1999) study, the COV of dynamic effect is assumed to be same as that of girder bridge i.e., $V_{\hat{\theta},IM} = 0.09$. The COV ($V_{IM}$) of dynamic effect can be calculated as follows:

$$V_{IM} = (1 + IM) * V_{\hat{\theta},IM} \tag{3.7}$$

Chapter 4

Maximum Live Load Effect based on Axle Weight Spectrum

4.1 Development of Axle Weight Spectrum

Due to the relative short span, the safety of a culvert is controlled by the axle weight instead of the gross vehicle weight. As a result, uncertainty characteristic due to random vehicle passages can be different from those in bridges. To model the uncertainty characteristics, we relied on the axle weight spectrum reported in NCHRP Report 683 (Sivakumar, et al., 2011). Table 4.1 provides the axle load statistic used in the present study. The spectrum is based on data from WIM Site 9926 in Florida. To generate Table 4.1, the raw WIM data have been processed following the protocol in NCHRP Report 683 (Sivakumar, et al., 2011), and the dynamic effect has been removed. For simplicity, only single axle and tandem configurations are considered as they account for the great majority among all vehicle passage events.

Table 4.1: Axle weight group statistic (WIM site data)

Statistic	**Single Axle**	**Tandem**
Count (N)	2,986,536	3,293,111
Mean total weight (kip)	10.831	21.773
Standard deviation of total weight (kip)	3.494	9.847

4.2 Structural Frame Analysis for Culverts

The structural frame analysis is recommended in (AASHTO, 2019) for preliminary structural analysis of RC box culverts. In this method, a 2D frame model is created, and the vehicle load is distributed through the backfill based on the LRFD load distribution model and applied to the top slab of a culvert as a uniformly distributed load. The length and magnitude of this uniformly distributed load are calculated as per the equations in Table 2.1. As mentioned in Chapter 3, this model serves two purposes: (a) identifying critical locations for different load effects and sections, and (b) calculating the maximum live load effect induced by moving loads. The frame model is assumed to be made up of linear elastic members. To establish structural nodes within this model, we set the coordinate origin at the bottom left corner of a culvert. Subsequently, we label the nodes systematically as follows:

- Starting from the coordinate origin, label the slab-wall joints with a 1000 interval in a counter clock wise direction.
- To differentiate wall nodes and elements from slab nodes and elements, add a prefix 10000 to the previously defined wall nodes and elements.

Figure 4.1 illustrates a typical 2D frame model of a culvert, developed using OpenSeesPy (Zhu, et al., 2018), a Python interpreter of the popular structural analysis script OpenSees (McKenna, 2011). It is important to note that Figure 4.1 is provided for explanatory purposes. In the study, 100 elements were typically utilized for walls and each slab cell. As per (AASHTO, 2018), vertical loading shall be balanced by an uplift reaction applied to the bottom slab, as shown in Figure 4.1(c).

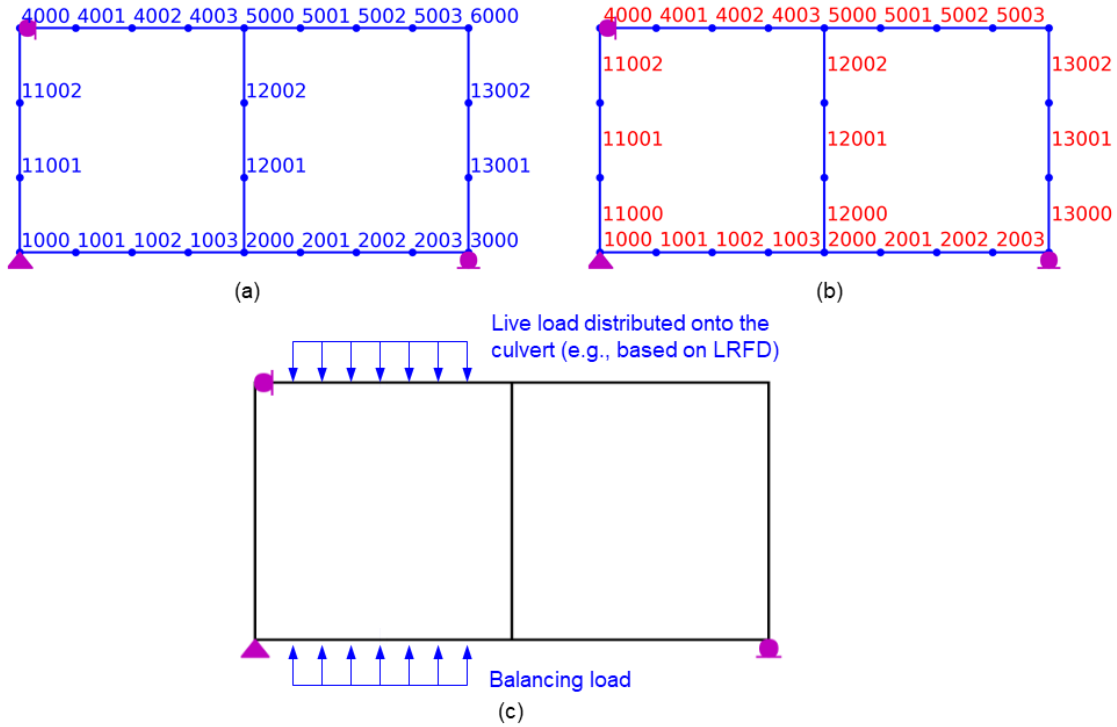

Figure 4.1: Structural analysis model: (a) nodes, (b) elements, (c) load pattern

4.3 Uncertainty Quantification of Live Load Effect based on Axle Weight Spectrum

Based on the general description in Chapter 3, Figure 4.2 shows the detailed the flowchart for uncertainty quantification of live load effects under axle loads. These steps are illustrated for Culvert 31 in Table 1.1 with 4 ft backfill and the load spectrum in Table 4.1. The 2D frame model is created and analyzed based on techniques in Section 4.2. Steps in the flowchart are described in detail in the following subsections.

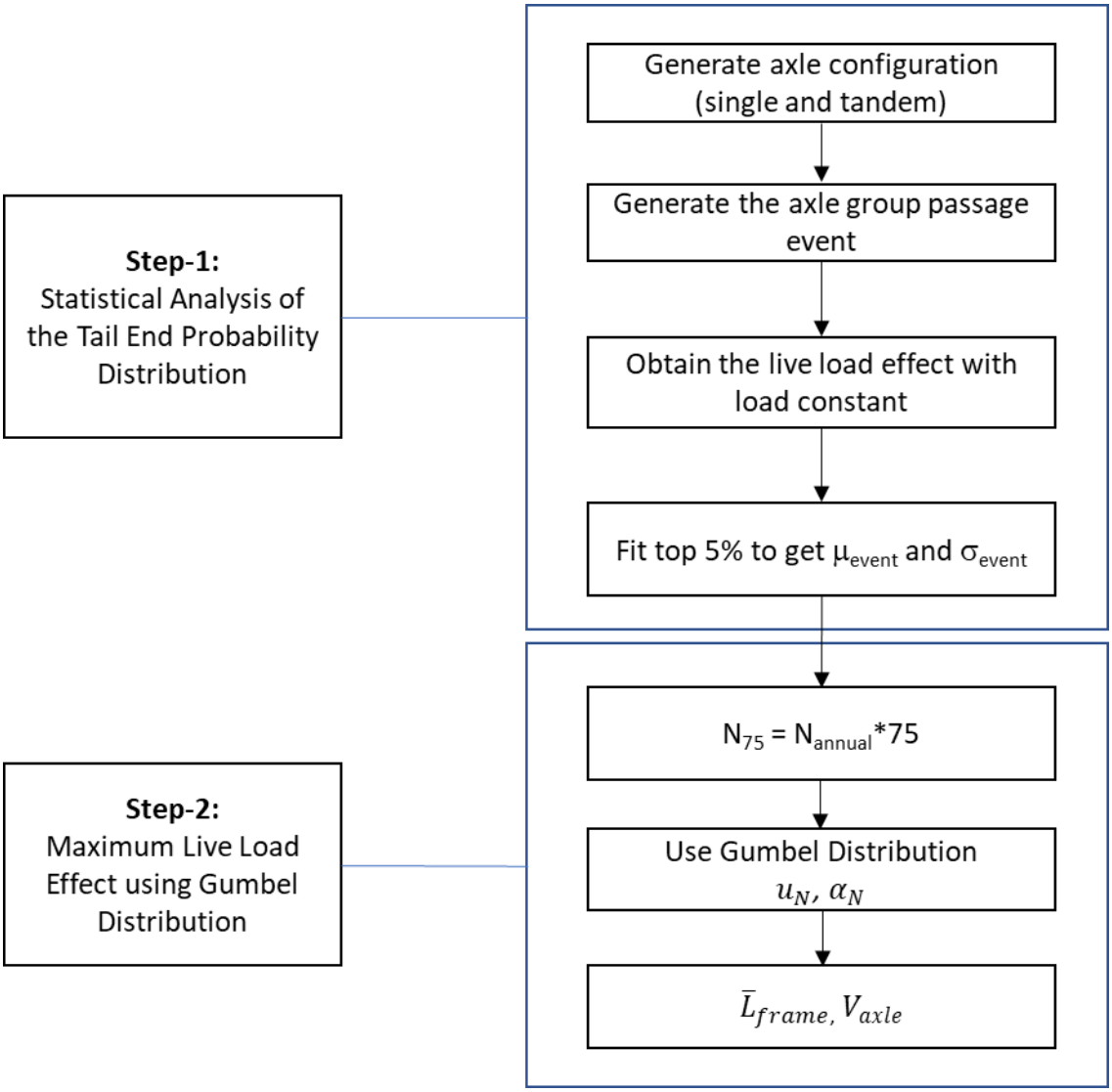

Figure 4.2: Flowchart showing the statistical analysis on axle weight effect

4.3.1 Statistical Analysis of the Tail End Probability Distribution

In this step, 2D frame analysis is first conducted to determine the load effects under (a) a unit load of 1 kip distributed over two tire contact areas and (b) two-unit loads, spaced 4 feet apart, distributed over four tire contact areas. These load effects are termed load constants under single and tandem axles for (a) and (b), respectively. For instance, $m_{S2,single} = 0.1279$ k-ft/ft/k for moment at Section 2 under load case (a). Similarly,

other load constants can be determined, and they are reported in Table 4.2 for the example culvert.

Table 4.2: Load constants for the example culvert (Culvert 31 with 4 ft backfill)

Axle Pattern	Bending moment constant (k-ft/ft/k)			Shear force constant ((k/ft/k)	
	m_{S1}	m_{S2}	m_{S3}	v_{S1}	v_{S3}
Single	0.05179	0.12799	0.09774	0.06033	0.06574
Tandem	0.08579	0.19426	0.16475	0.09258	0.10529

After load constants are determined, a sufficient number (e.g., 10000) of axle weight samples are generated based on the axle spectrum in Table 4.1. For each axle sample, the axle weight is multiplied with the appropriate load constant to obtain the load effect under that sample axle weight. For instance, if the generate sample is a single axle weighing 32 kips, the midspan bending moment (e.g., moment at Section 2) is (32 kip × 0.12799 k-ft/ft/k =) 4.0956 k-ft/ft. Note that for tandem configuration, weight of one axle should be substitute to the aforementioned procedure.

For the example culvert, Figure 4.3 shows the sample load effects (i.e., moment at Section 2) generated with the process described above, and they are presented in the form of a normal probability plot. It becomes evident that the entire dataset does not conform to a normal distribution, as indicated by the curve's lack of alignment with a straight line on the plot. However, Figure 4.3 reveals that the upper 5% of the data exhibits behavior

resembling that of a hypothetical normal distribution's tail end. The upper 5% data correspond to the load effects caused by heavy axle weight relevant to maximum load projection described subsequently. A linear fit is applied on this normal probability plot to the upper 5% data. The linear fit yields two important parameters: i.e., a slope and an intercept denoted herein as m and n, respectively. Based on these parameters, the mean weight (μ_{event}) in an axle passage event can be calculated as $\mu_{event} = -n/m.$; the standard deviation (σ_{event}) is $1/m$.

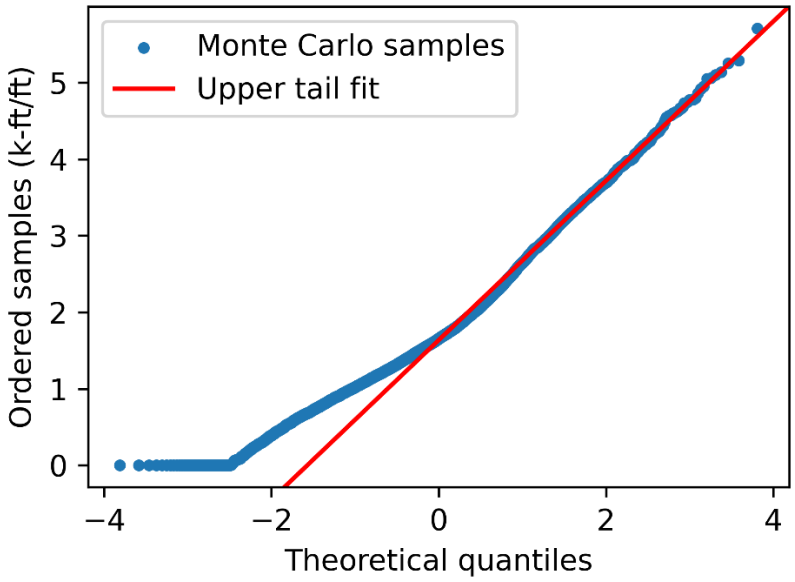

Figure 4.3: Probability plot of mid-span moment samples and its upper 5% tail fit

4.3.2 Maximum Live Load Effect using Gumbel Distribution

To project the live load effects from one axle passage event to the maximum load effect within a 75-year timeframe, the Gumbel distribution is used. Gumbel distribution provides the behavior of extreme events in various systems and serves as a useful tool for risk assessment, reliability analysis, and decision-making (Nowak & Collins, 2012).

Below is the procedure to calibrate the parameters of a Gumbel distribution representing the maximum live load effect over the 75-year culvert design period (Sivakumar, et al., 2011):

1. Estimate the number of events per day (n_{day}), and determine the total number of events (N) within 75 years: $N = n_{day} \times 365 \times 75$.
2. Compute the mode u_N of the Gumbel distribution (i.e., the most probable value) using the expression below:

$$u_N = \mu_{event} + \sigma_{event}\left[\sqrt{2ln\,(N)} - \frac{ln(ln(N))+ln\,(4\pi)}{2\sqrt{2ln\,(N)}}\right] \quad (4.1)$$

3. Calculate the dispersion coefficient α of the Gumbel distribution using the expression below

$$\alpha_N = \frac{\sqrt{2\ln\,(N)}}{\sigma_{event}} \quad (4.2)$$

Based on the mode and dispersion coefficient, the mean and standard deviation of the 75-year maximum load effect can be expressed as (Sivakumar, et al., 2011) :

$$\bar{L}_{frame} = u_N + \frac{0.577216}{\alpha_N} \quad (4.3a)$$

$$V_{axle} = \frac{\pi}{\bar{L}_{frame}\sqrt{6}\alpha_N} \quad (4.3b)$$

Note that the total COV of L_{frame} needs to also consider the data and site variability related to the WIM data. Specifically. Equation 3.4 is used to convert V_{axle} to $V_{L,frame}$.

4.4 Results from 2D Frame Analysis Under Projected Axle Loads

The procedures described in Section 4.3 are implemented for all the representative culverts in Table 1.1 and their load effects of interest are presented in Table 4.3. The projected mean and COV of 75-year maxima are listed in Table 4.3. It can be observed that uncertainty due to live load is relatively low. Therefore, uncertainty associated with the axle weight spectrum seems to be dominated by variabilities due to WIM sites and data amount.

Table 4.3: Mean ($\bar{L}_{frame}$) and COV (V_{axle}) of live load effects due to axle weight spectrum

Culvert ID	D (ft)	Mean of M_{S1}	COV of M_{S1}	Mean of M_{S2}	COV of M_{S2}	Mean of M_{S3}	COV of M_{S3}	Mean of V_{S1}	COV of V_{S1}	Mean of V_{S3}	COV of V_{S3}
1	4	3.524	0.027	5.661	0.027	3.524	0.027	3.483	0.027	3.550	0.027
2	4	2.979	0.027	6.203	0.027	2.979	0.027	3.481	0.027	3.547	0.027
3	4	2.570	0.027	6.612	0.027	2.570	0.027	3.480	0.027	3.546	0.027
4	4	2.250	0.027	6.932	0.027	2.250	0.027	3.479	0.027	3.544	0.027
5	4	3.610	0.027	8.633	0.027	3.610	0.027	3.923	0.027	3.989	0.027
6	4	3.080	0.027	9.154	0.027	3.080	0.027	3.917	0.027	3.983	0.027
7	4	3.422	0.027	8.910	0.027	3.422	0.027	3.926	0.027	3.991	0.027
8	4	3.072	0.027	9.254	0.027	3.072	0.027	3.922	0.027	3.987	0.027
9	4	4.517	0.027	10.986	0.027	4.517	0.027	4.256	0.027	4.321	0.027
10	4	3.997	0.027	11.490	0.027	3.997	0.027	4.247	0.027	4.312	0.027
11	4	5.075	0.027	10.659	0.027	5.075	0.027	4.276	0.027	4.341	0.027
12	4	4.694	0.027	11.024	0.027	4.694	0.027	4.269	0.027	4.333	0.027
13	4	6.518	0.027	12.125	0.027	6.518	0.027	4.527	0.027	4.592	0.027
14	4	5.739	0.027	12.861	0.027	5.739	0.027	4.510	0.027	4.575	0.027
15	4	6.882	0.027	11.941	0.027	6.882	0.027	4.530	0.027	4.594	0.027
16	4	6.367	0.027	12.424	0.027	6.367	0.027	4.518	0.027	4.582	0.027
17	4	9.060	0.027	21.038	0.027	9.060	0.027	4.921	0.027	4.980	0.027
1	8	1.763	0.027	2.829	0.027	1.763	0.027	1.738	0.027	1.774	0.027
2	8	1.490	0.027	3.103	0.027	1.490	0.027	1.738	0.027	1.774	0.027
3	8	1.285	0.027	3.309	0.027	1.285	0.027	1.738	0.027	1.774	0.027

4	8	1.125	0.027	3.470	0.027	1.125	0.027	1.738	0.027	1.774	0.027
5	8	1.913	0.027	4.520	0.027	1.913	0.027	2.050	0.027	2.092	0.027
6	8	1.631	0.027	4.803	0.027	1.631	0.027	2.050	0.027	2.092	0.027
7	8	1.825	0.027	4.692	0.027	1.825	0.027	2.063	0.027	2.105	0.027
8	8	1.637	0.027	4.880	0.027	1.637	0.027	2.063	0.027	2.105	0.027
9	8	2.610	0.027	6.134	0.027	2.610	0.027	2.381	0.027	2.428	0.027
10	8	2.309	0.027	6.436	0.027	2.309	0.027	2.381	0.027	2.428	0.027
11	8	2.958	0.027	5.970	0.027	2.958	0.027	2.405	0.027	2.452	0.027
12	8	2.738	0.027	6.190	0.027	2.738	0.027	2.405	0.027	2.452	0.027
13	8	3.974	0.027	6.999	0.027	3.974	0.027	2.641	0.027	2.689	0.027
14	8	3.505	0.027	7.464	0.027	3.505	0.027	2.639	0.027	2.687	0.027
15	8	4.231	0.027	6.925	0.027	4.231	0.027	2.660	0.027	2.708	0.027
16	8	3.919	0.027	7.232	0.027	3.919	0.027	2.658	0.027	2.706	0.027
17	8	6.297	0.027	13.648	0.027	6.297	0.027	3.257	0.027	3.304	0.027
18	4	1.033	0.027	2.252	0.027	2.798	0.027	2.106	0.027	2.562	0.027
19	4	0.684	0.027	2.460	0.027	2.862	0.027	2.063	0.027	2.613	0.027
20	4	0.494	0.027	2.574	0.027	2.889	0.027	2.040	0.027	2.637	0.027
21	4	1.041	0.027	4.169	0.027	3.670	0.027	2.649	0.027	3.224	0.027
22	4	1.191	0.027	4.217	0.027	3.722	0.027	2.698	0.027	3.254	0.027
23	4	0.948	0.027	4.362	0.027	3.718	0.027	2.675	0.027	3.276	0.027
24	4	3.399	0.027	5.386	0.027	5.229	0.027	3.405	0.027	3.805	0.027
25	4	2.795	0.027	5.742	0.027	5.110	0.027	3.358	0.027	3.845	0.027
26	4	2.359	0.027	5.998	0.027	5.028	0.027	3.324	0.027	3.875	0.027
27	4	2.031	0.027	6.192	0.027	4.966	0.027	3.298	0.027	3.897	0.027
28	4	3.307	0.027	7.834	0.027	6.577	0.027	3.761	0.027	4.299	0.027
29	4	3.585	0.027	7.808	0.027	6.700	0.027	3.794	0.027	4.302	0.027
30	4	3.930	0.027	7.793	0.027	6.879	0.027	3.847	0.027	4.329	0.027
31	4	3.540	0.027	8.017	0.027	6.799	0.027	3.821	0.027	4.345	0.027
32	4	4.152	0.027	9.999	0.027	8.163	0.027	4.099	0.027	4.616	0.027
33	4	3.615	0.027	10.303	0.027	8.052	0.027	4.066	0.027	4.631	0.027
34	4	4.795	0.027	9.932	0.027	8.448	0.027	4.163	0.027	4.630	0.027
18	8	0.512	0.027	1.116	0.027	1.615	0.027	1.044	0.027	1.323	0.027
19	8	0.339	0.027	1.219	0.027	1.680	0.027	1.023	0.027	1.354	0.027
20	8	0.245	0.027	1.276	0.027	1.710	0.027	1.011	0.027	1.370	0.027
21	8	0.515	0.027	2.063	0.027	2.638	0.027	1.311	0.027	1.715	0.027
22	8	0.589	0.027	2.087	0.027	2.670	0.027	1.335	0.027	1.727	0.027
23	8	0.469	0.027	2.159	0.027	2.700	0.027	1.324	0.027	1.741	0.027
24	8	1.706	0.027	2.703	0.027	3.306	0.027	1.704	0.027	1.968	0.027

25	8	1.401	0.027	2.885	0.027	3.348	0.027	1.681	0.027	1.995	0.027
26	8	1.180	0.027	3.015	0.027	3.377	0.027	1.664	0.027	2.013	0.027
27	8	1.014	0.027	3.114	0.027	3.399	0.027	1.652	0.027	2.027	0.027
28	8	1.752	0.027	4.114	0.027	3.952	0.027	1.961	0.027	2.295	0.027
29	8	1.913	0.027	4.116	0.027	3.986	0.027	1.987	0.027	2.305	0.027
30	8	2.099	0.027	4.104	0.027	4.025	0.027	2.014	0.027	2.315	0.027
31	8	1.889	0.027	4.229	0.027	4.017	0.027	2.001	0.027	2.328	0.027
32	8	2.407	0.027	5.594	0.027	4.828	0.027	2.280	0.027	2.650	0.027
33	8	2.094	0.027	5.779	0.027	4.771	0.027	2.262	0.027	2.667	0.027
34	8	2.803	0.027	5.571	0.027	5.026	0.027	2.329	0.027	2.668	0.027

Note: The bending moment ($\boldsymbol{M_{S1}}$, $\boldsymbol{M_{S2}}$, $\boldsymbol{M_{S3}}$) and shear force ($\boldsymbol{V_{S1}}$, $\boldsymbol{V_{S3}}$) are calculated in k-ft/ft and k/ft, respectively.

Chapter 5

Finite Element Modeling for Live Load Distribution

5.1 Finite Element Modeling of RC Box Culvert

Culverts are buried structures that can interact with the surrounding soil. The FE analysis of a soil-culvert system follows the same procedures established in NCHRP Report 647 (Petersen, et al., 2010). Though both 2D and 3D models were investigated in that report, 3D FE models are developed herein due to their capacity of reflecting load distribution in all three directions in the soil domain (i.e., depth, culvert span, and culvert length directions).

The dimensions of the soil domain need to be sufficiently large in all directions so that the load distribution is not affected by the boundary conditions of a soil-culvert system. Additionally, it is assumed that the culvert has sufficient length in the transverse direction (i.e., the culvert length direction) so that the load distribution in that direction can be fully developed. Therefore, the soil domain has a depth of 30 ft (in the direction of culvert height), a width of 60 ft (in the direction of culvert span), and a length of 36 ft (in the direction of culvert length). An RC culvert penetrates through the entire length of the soil domain and, therefore, also has a length of 36 ft (Petersen, et al., 2010). Moreover, it is considered that the center of an axle is located in the middle plane of a culvert (and the soil domain) along its length direction. Therefore, only a half model with a length of 18 ft is needed for the FE analysis due to symmetry of geometric and loading conditions. It should be noted that when using this half-model, only half of the total axle loads should

be applied. Figure 5.1 (a) and Figure 5.1(b) shows the typical FE models of one- and two-cell culverts, respectively

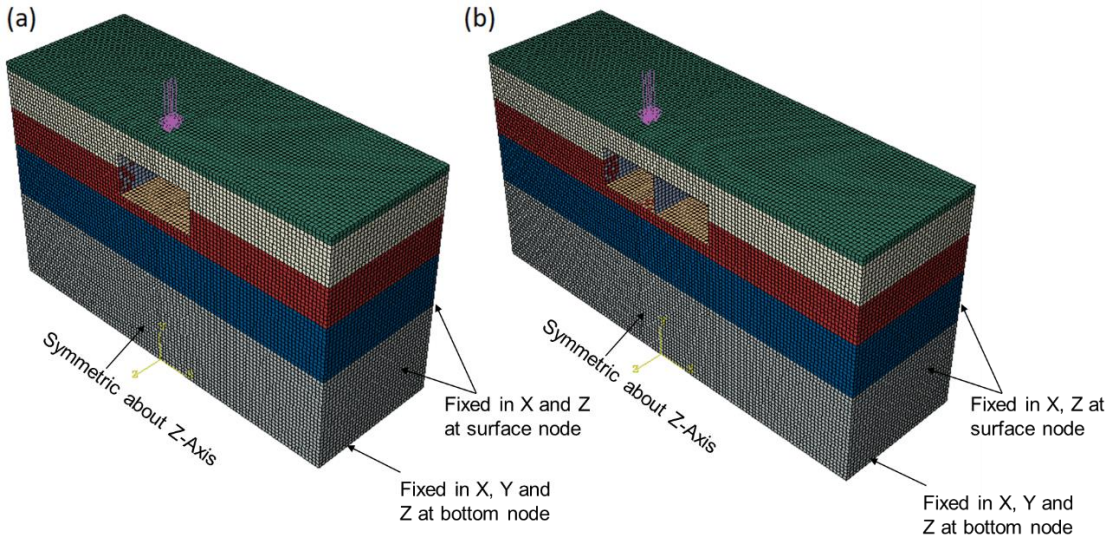

Figure 5.1: Representation of typical FE culvert model (a) one cell (b) two cell

5.1.1 Structural Modeling

The culvert is modeled using the 4-node doubly curved shell element with reduced integration and hourglass control. The RC box culvert's Young's modulus and density are 4,030,000 psi and 150pcf, respectively. The constitutive behavior of the structure is considered in the linear elastic range because linear elasticity simplifies the analysis significantly without losing much accuracy in the predicted load effects (Petersen, et al., 2010). The linear behavior of a structure allows for the simple comparison between 2D frame and FE models under unit loads, because this ratio stay constant regardless of the axle weight under consideration (no need to re-calculate ratio from two models under different axle weights). This convenience is not available in the case of nonlinear behavior of a structure.

In the analysis of a culvert using ABAQUS, different reference surfaces for shell elements can be employed. Herein, the following reference surfaces are utilized to better reflect the contact between the culvert and the surrounding soil:

- The outer surface is used as the reference surface of shell elements for slabs and side walls. This is because the outer surface of the slab and the culvert is typically in direct contact with the surrounding soil. By referencing to the outer surface, the analysis can accurately represent the interaction and contact between the culvert structure and the surrounding soil.
- The middle surface is chosen as the reference surface of shell elements for modeling the internal wall in 2-cell culverts. The internal wall primarily serves to separate the two cells of the culvert. Since it does not directly interact with the soil, using the middle surface ensures that the culvert can have symmetrical responses under symmetrical loads.

5.1.2 Soil Modeling

For the modeling of the soil, 8-node linear brick element with reduced integration and hourglass control is used. For culverts, the backfill soil is typically well graded or gravelly sand at 85% standard compaction (SW85). Table 5.1 provide the linear-elastic properties of the SW85 soil with constant density of 120pcf for all layers. The second type of soil model representing inorganic silts and fine sand at 85% standard compaction (ML85), as listed in Table 5.2, is also considered in the analysis to understand the effect of backfill property on load distribution. Both soil models are assumed to be linear elastic. The modulus of elasticity of the soil is increasing from top to bottom, which

reflects the consolidated soil as the depth increases. Moreover, the use of linear elastic soil is also supported by previous research studies on RC culverts ((Petersen, et al., 2010); (Wood, et al., 2016)). They indicate that the soil in a culvert-soil system mostly behaves in the linear elastic range under 32-kip axle load.

Table 5.1: Parameters for soil properties (SW85) (Petersen, et al., 2010)

Depth (ft)	**Elastic modulus, E (psi)**	**Poisson's Ratio (ν)**
0-1	1300	0.26
1-6	2100	0.21
6-11	2600	0.19
11-30	3300	0.19

Table 5.2: Parameters for soil properties (ML85) (Petersen, et al., 2010)

Depth (ft)	**Elastic modulus, E (psi)**	**Poisson's Ratio (ν)**
0-1	600	0.25
1-6	700	0.24
6-11	800	0.23
11-30	850	0.30

5.1.3 Soil Culvert Interface Modeling

To simulate the interaction between the culvert and the soil, a rigid contact model is employed. This model incorporates a contact surface consisting of two distinct surfaces: one designated as the master surface and the other as the slave surface, as illustrated in Figure 5.2. It is important to note that these contact surfaces can exhibit both rigidity and flexibility. In this context, the rigid body serves as the slave surface, while the flexible body functions as the master surface. This means that the master surface can transmit loads to the slave surface, but not vice versa. In this soil-culvert problem transfer of force

occurs from the flexible body to the rigid body. Consequently, in this analysis, the soil is considered to act as the master surface, while the culvert is regarded as the slave surface, following the principles outlined in (ABAQUS, 2019).

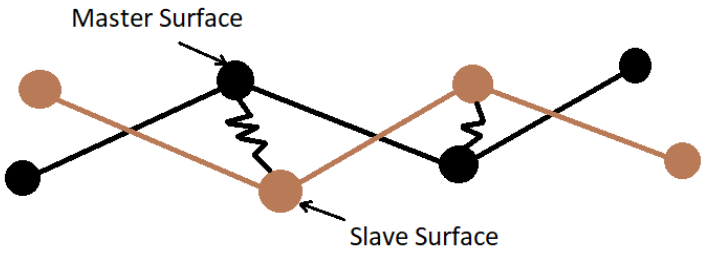

Figure 5.2: Master and slave surface coupling

5.2 Automation of FE Modeling

3D models of culverts are created automatically for all typical culverts using the ABAQUS Python scripts. Prior to the model creation, the structural frame model is first created, as described in Section 4.2, to locate the critical location of the axles that causes the maximum load effect under moving loads. This location is further used in the 3D finite element model of soil-culvert system within the ABAQUS python script. In the python script of ABAQUS, the tire pressure was applied at the top of the soil and response was calculated at the various critical location of the culvert. Figure 5.3 shows the basic steps of modeling of RC box culvert using the ABAQUS script.

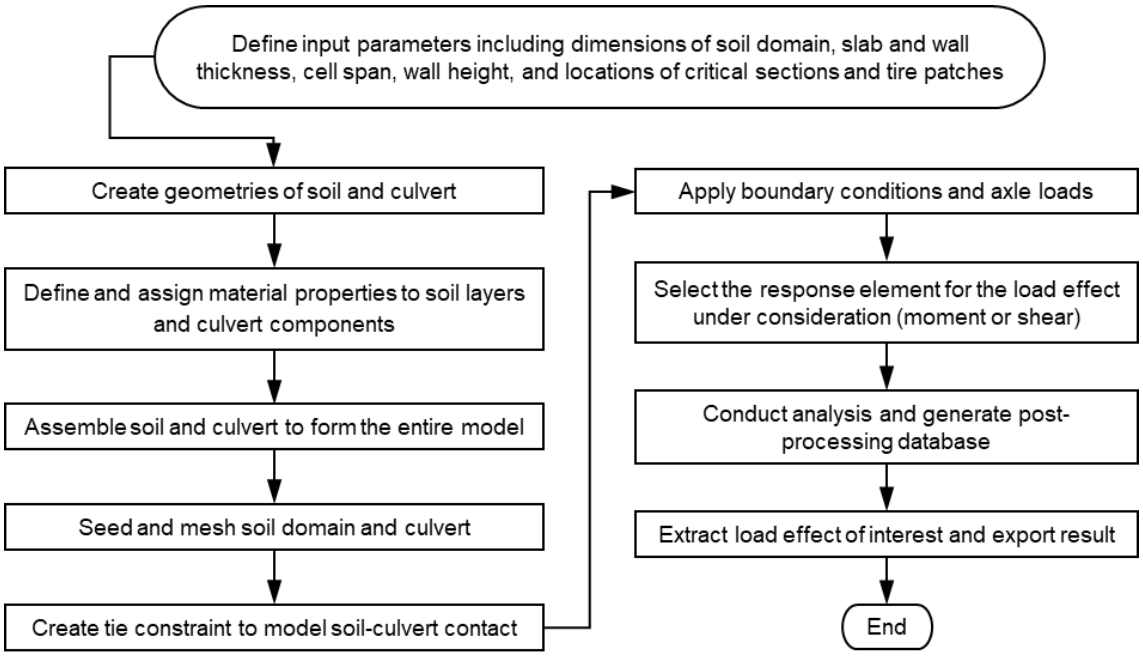

Figure 5.3: Flowchart of automated FE analysis using ABAQUS scripting interface

5.3 Finite Element Model Validation

To validate the modeling techniques, FE analysis of a one-cell culvert is conducted, and the bending moment within the culvert is compared with the FE analysis results reported in (Petersen, et al., 2010) . The dimension of the modeled culvert is 4 ft (clear width) by 4 ft (clear height), and the backfill depth is also 4 ft. Based on the ASTM standard specification (ASTM C789-95, 1995), the wall and slab thicknesses are both 5 in. The culvert is subjected to an axle load of 50.544 kips on the road surface right above the culvert midspan. The axle load has two tire contact areas each of 10 in (traffic direction) by 20 in (axle direction), resulting in a 0.126 ksi pressure on each patch ((Petersen, et al., 2010); (AASHTO, 2019)). Under this load pattern, only a quarter model is needed by capitalizing on the symmetry of geometric and load conditions.

Figure 5.4 shows the FE model used for the validation. On the symmetry plane YZ, the translational displacement in X direction and the rotational displacement around Z direction are restrained. Similarly, the translational displacement in Z direction and the rotational displacement around X direction are restrained on the symmetry plane XY. One fourth of the total axle load, i.e., 12.636 kips, is applied 3 ft (half axle length) away from the plane XY, as illustrated in Figure 5.4. In line with the principles mentioned in Section 5.1, the depth and width of the soil domain in the quarter model are 14.5 ft and 12 ft, respectively, which are identical to the values used in the NCHRP report 647 (Petersen, et al., 2010). Different colors stand for materials with different elastic moduli; the point load is presented for illustration purposes only; the axle load is actually applied as a patch load based on a half of the tire contact area. The soil properties used herein are the same as those reported in the Table 5.1.

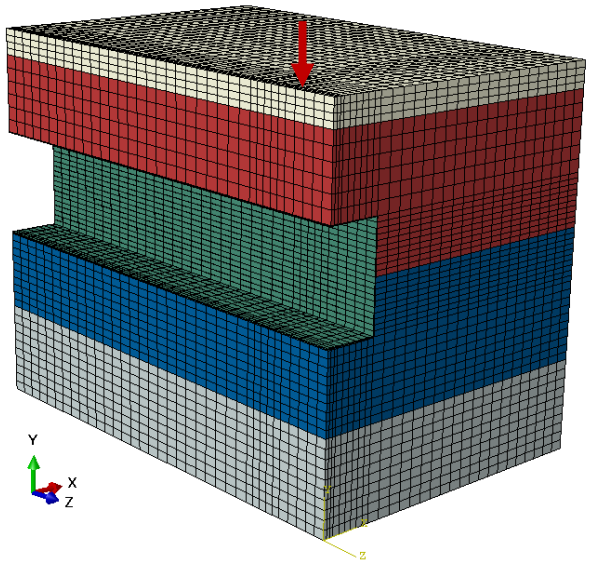

Figure 5.4: FE model of the culvert used for validation

Error! Reference source not found. shows the bending moment values within the analyzed culvert. The values reported in (Petersen, et al., 2010) are also presented for

comparison. In Figure 5.5(a), the mid-surface of shell elements is used as the reference surface in order to be consistent with the original NCHRP report 647. In Figure 5.5(b), the reference surface for the shell elements is selected based on the rules mentioned previously (i.e., outer surface). From the comparison, it can be found that the modeling techniques used in this task can deliver results in good agreement with those in the NCHRP report 647. The close resemblance is especially evident in and near the top slab, where the focus of the present study lies. It should be noted that the (Petersen, et al., 2010) used FLAC-3D, in which finite difference is used in lieu of finite element analysis. This might explain the subtle differences obtained in Figure 5.5(a). Furthermore, the discrepancy in Figure 5.5(b) suggests that properly selecting the reference surface does have a noticeable impact on the bending moment values, especially for the midspan moment relevant to the design. In this study, the outer surface is used due to reasons previously in section 5.1.1.

In summary, we consider that the FE modeling techniques are successfully validated. The validated modeling techniques are valuable tools for a comprehensive investigation into the behavior of the soil-culvert system under different load conditions and analytical approaches.

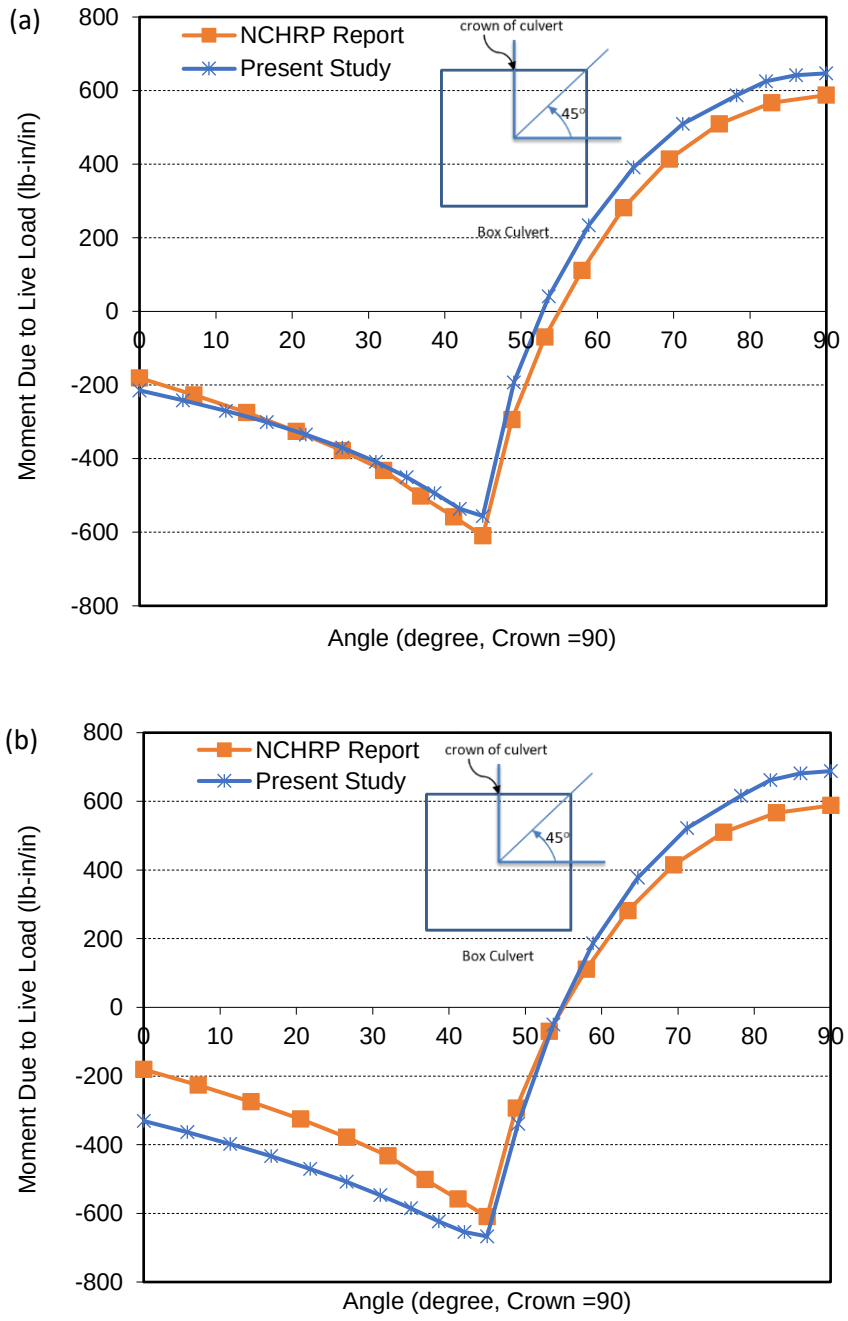

Figure 5.5: Bending moment within the investigated culvert: (a) reference surface = mid-surface, and (b) reference surface = outer-surface

5.4 Pressure Distribution with Varying Soil Properties and Tire Location

In this section, the pressure distribution across the culvert is computed by applying a 1-kip single axle load in a linear elastic culvert-soil system. Due to linear linearity, load

effects in culverts from an axle weight of 32 kips can be obtained by the load effect under 1 kip of the same axle configuration with multiplied by 32. Culvert 19 in Table 1.1 is selected for this analysis. To capture the soil's impact on pressure distribution, two types of soil are examined.

The first type of soil analyzed is well-graded or gravelly sand at 85% standard compaction (SW85), as listed in Table 5.1. The second type is inorganic silts and fine sand at 85% standard compaction (ML85), as listed in Table 5.2. The analysis involves moving the tire patch load from the external wall toward the internal wall with a 2-ft spacing. Pressure distribution is then extracted in the soil layer just above the culvert.

Figure 5.6 illustrates the contour of pressure distribution in the culvert for a 4-ft backfill depth. From the figure, it can be seen that live load distribution is less uniformly distributed when the axle location is close to the exterior (Figure 5.6(a)) or internal wall (Figure 5.6(c)). On the other hand, when the axle is near the cell midspan, the uniformly distributed load from the LRFD distribution model more closely matches the results from FE analysis (Figure 5.6(b)). A similar observation can be made for an 8-ft backfill depth, as shown in Figure 5.7, with a lower concentration of pressure distribution. Furthermore, the pressure distribution in the soil layer is spread over a larger area of soil for the 8-ft backfill depth.

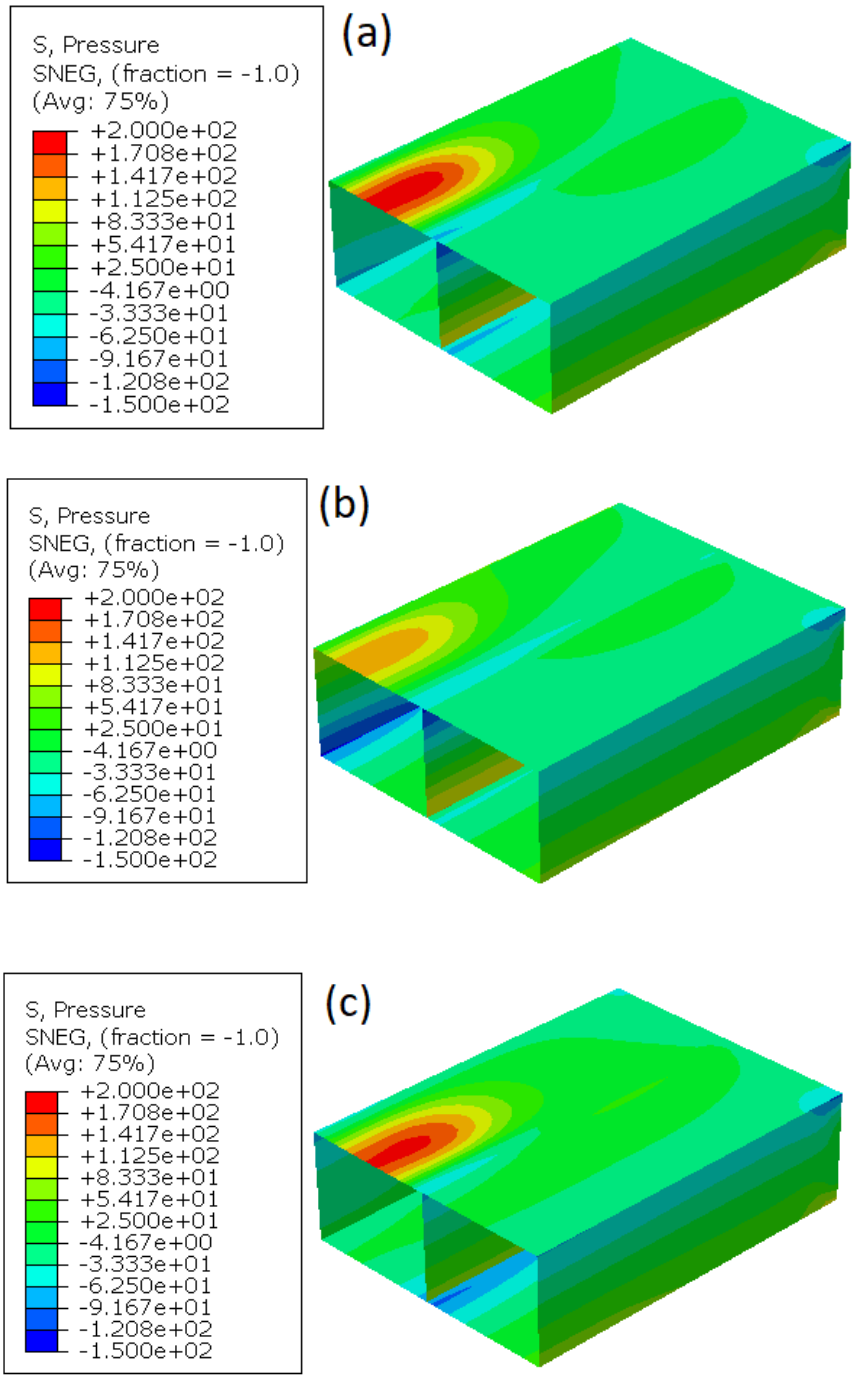

Figure 5.6: Soil pressure (lb/ft^2) distribution in culvert for SW85 soil under the 4ft backfill depth when the tire load (a) at external wall; (b) 2ft away from external wall and (c) 4ft away from external wall

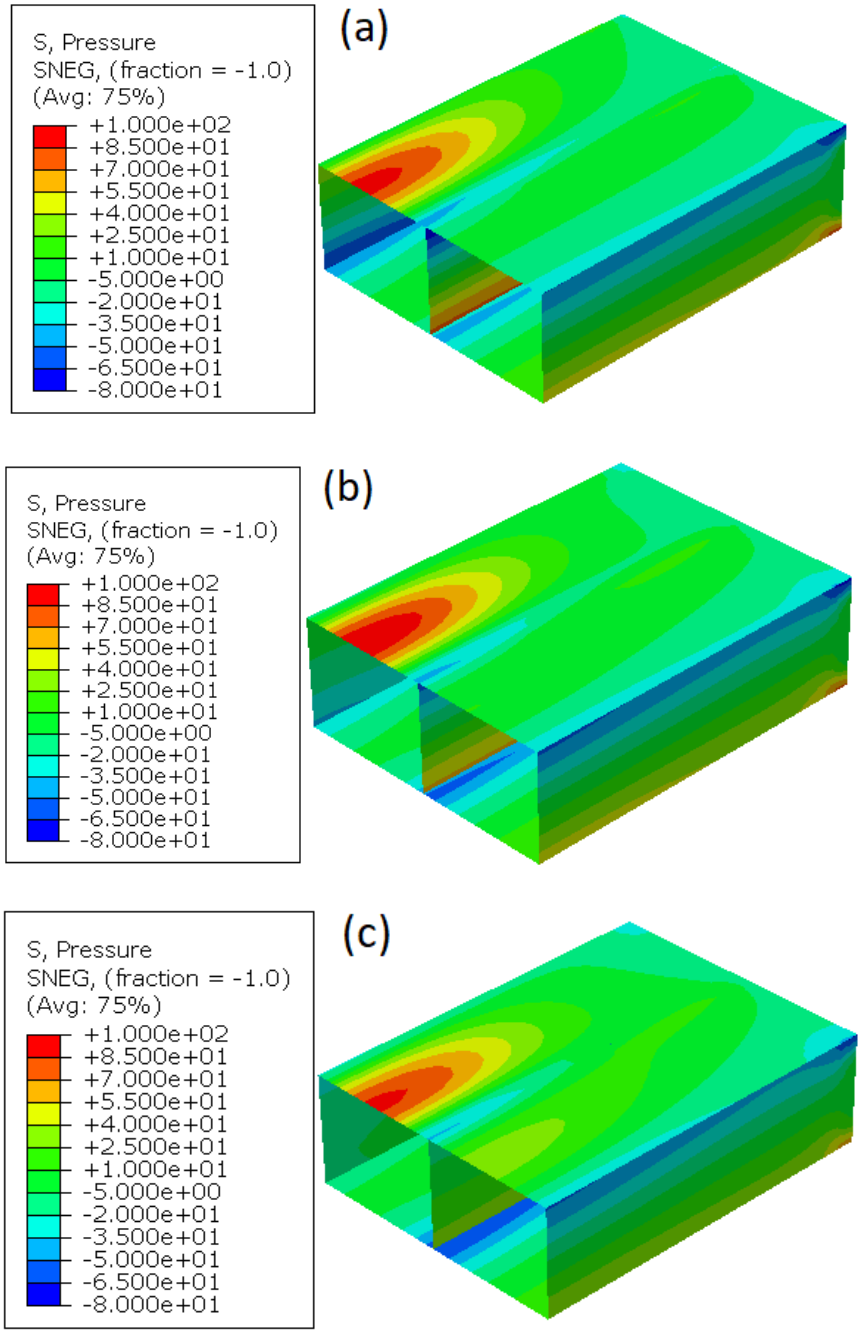

Figure 5.7: Soil pressure (lb/ft^2) distribution in culvert for SW85 soil under the 8ft backfill depth when the tire load (a) at external wall; (b) 2ft away from external wall and (c) 4ft away from external wall

Figure 5.8(a) and (b) shows the pressure distribution in the culvert for the 4 ft backfill depth and 8 ft backfill depth, respectively. It can be observed that pressure on the soil

element just above the culvert is little higher (approximately 5%) in loose sand (ML85) with a low Young's modulus as compared to the dense sand (SW85) with high Young's modulus for the low backfill depth. Therefore, it can be said that material properties do not play a significant role in live load distribution over the culvert for the 4ft backfill depth. Furthermore, it is noteworthy that the peak pressure shifts with variations in tire locations. Additionally, there is an observable trend where the peak pressure increases as the tire approaches the mid-span and subsequently decreases slightly as it approaches the mid-wall. Moreover, for the 8ft backfill depth, the pressure on the culvert is more noticeably affected by the soil properties. These findings highlight the importance of considering both soil characteristics and tire placement in understanding and optimizing live load distribution over the culvert structure.

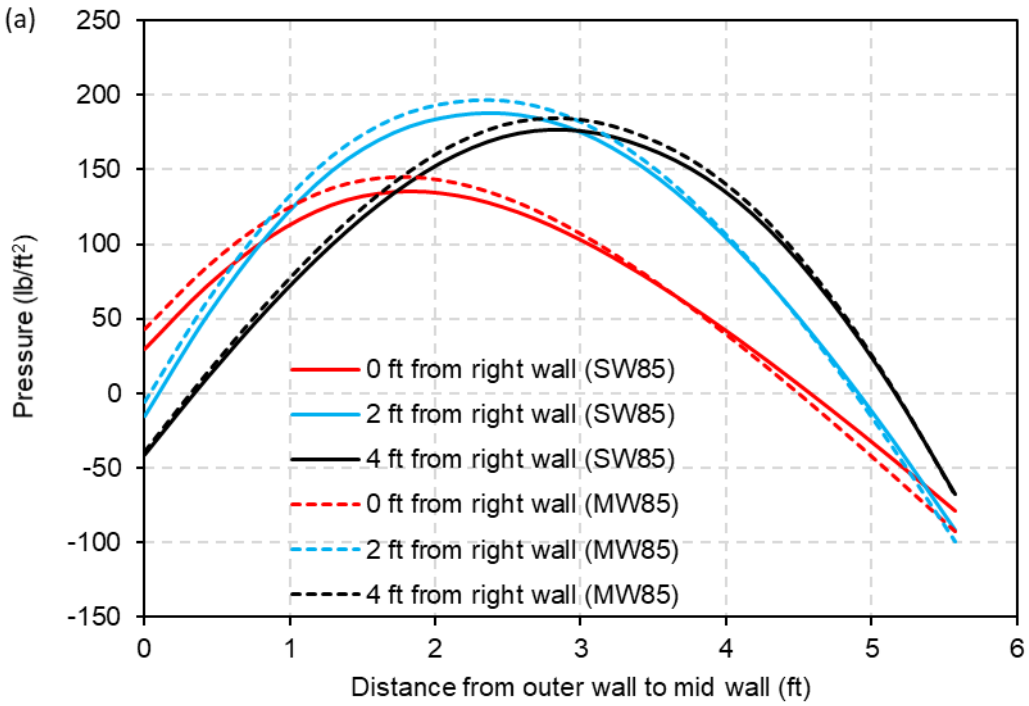

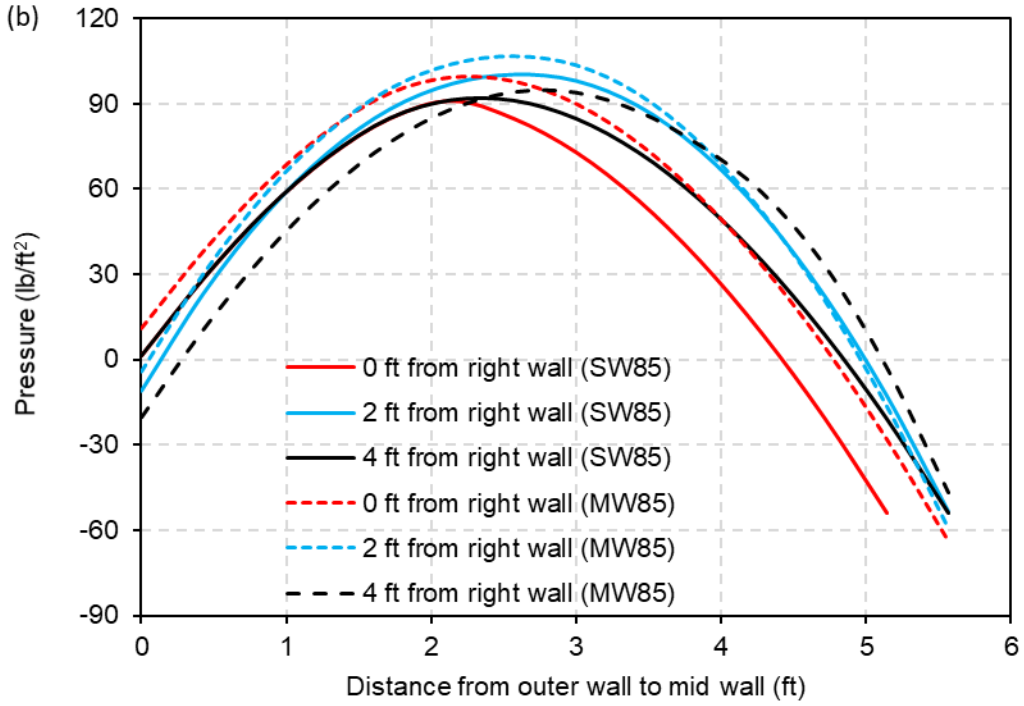

Figure 5.8: Pressure distribution at the top of culvert (a) 4ft backfill depth (b) 8ft backfill depth

5.5 Uncertainty quantification of load distribution model

In this section, factor λ_{LDS} defined in Chapter 3 is calibrated based on the structural frame model analysis and FE model analysis of culverts. For this, response at the critical locations of the culvert is determined as shown in Figure 1.1. The factor λ_{LDS} accounts the model error, i.e., error in calculating the response using the structural frame model compared to the 3D FE model of culverts. On the other hand, location of the tire on the soil surface in case of FE model is determined based on the structural frame model which may also lead to error in calculating the maximum response in FE model.

Utilizing the automated procedure outlined in Section 5.2, load effect factors are computed for all representative culverts employing both the plane frame model and the

3D FE model. Subsequently, the bending moment ratios and shear force ratio ($L_{max,frame}/L_{max,FEM}$) are derived for all culverts, serving as samples for uncertainty quantification.

Figure 5.9 shows the bending moment ratio obtained from both the FE model analysis and the structural frame model at sections S1, S2, and S3. In these results, factors such as cell span, backfill depth, axle configuration, and the number of cells is considered as potential explanatory variables for the variation in moment ratio. It is evident that the conservatism for the bending moment at the cell midspan (S2, positive bending moment) significantly increases with a larger cell span, exceeding 2 times that of the FE model. Conversely, the conservatism of the negative bending moment at sections S1 and S3 is higher compared to section S2, possibly due to low pressure on the culvert, as illustrated in Figure 5.8 and Figure 5.9. Hence, it can be inferred that when the tire is near the wall (either internal or external), the negative bending moment decreases in the FE model, particularly for high backfill depth. Additionally, it is noteworthy that for shorter spans, conservatism at sections S1 and S3 is comparatively high, exhibiting almost 4 times more negative bending moment in the structural frame model.

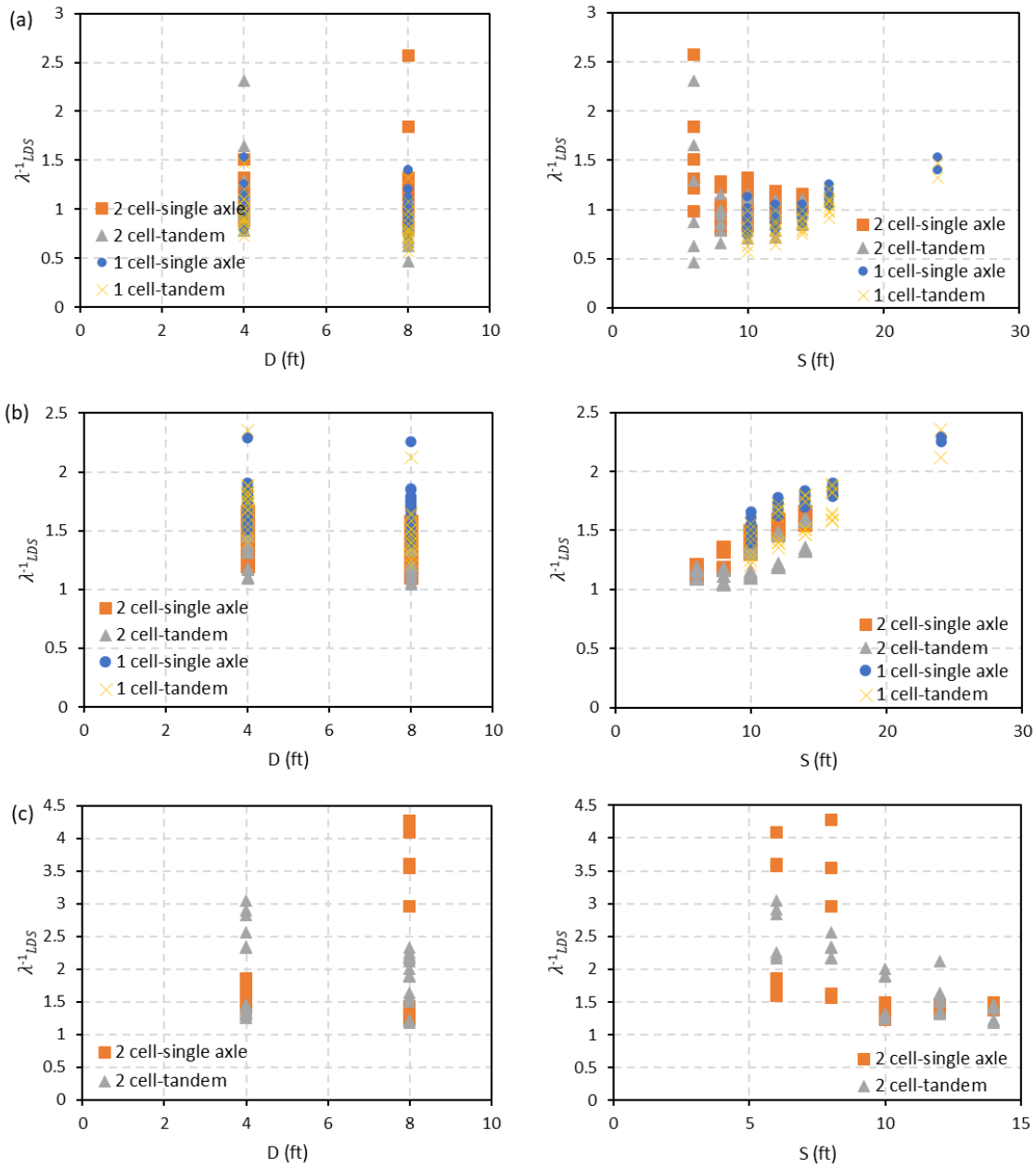

Figure 5.9: Comparison of structural frame model with FE model for bending moment at location (a) S1; (b) S2 and (c) S3

Figure 5.10 presents the shear force ratio at locations S1 and S3. It is evident that the shear force ratio slightly decreases with the increase in backfill depth at both locations. This indicates that the FE model produces higher shear force compared to the structural frame model. This discrepancy may be attributed to the structural frame model's utilization of the load as uniformly distributed, while the FE model incorporates the 3D real behavior of load distribution, following a triangular load distribution pattern.

To explain the high maximum shear force and low negative bending moment at section S3 in FE modeling, a conceptual model based on a continuous beam is analyzed as shown in Figure 5.11. The total magnitude of 1 kip is applied over the 5 ft span in two cases i.e., triangular and uniform load. Table 5.3 provides the comparison between the triangular loading and uniform loading distribution for the 2-span continuous beam of 10 ft span length. It can be observed that when the load is at the support and triangularly distributed, negative bending moment at the middle support is lower by 28.33% compared to the uniformly distributed load, and the shear force is slightly higher compared to the uniformly distributed load. Similar observation can be obtained when factor λ_{LDS} is calibrated using the FE and 2D structural frame model. Specifically, the FE model gives the lesser negative bending moment and higher shear force compared to the structural frame model. However, when the load is placed at the center of the beam, positive bending moment is increased by 13.29% under triangular load, which supports the present study finding. Motivated by a similar observation, (McGrath, et al., 2005) developed a live load distribution model for low fill culverts, revealing varying distribution widths for shear force, positive and negative bending. The live load

distribution width for the shear force was observed narrowest followed by the positive bending moment which is in line with finding from the present study.

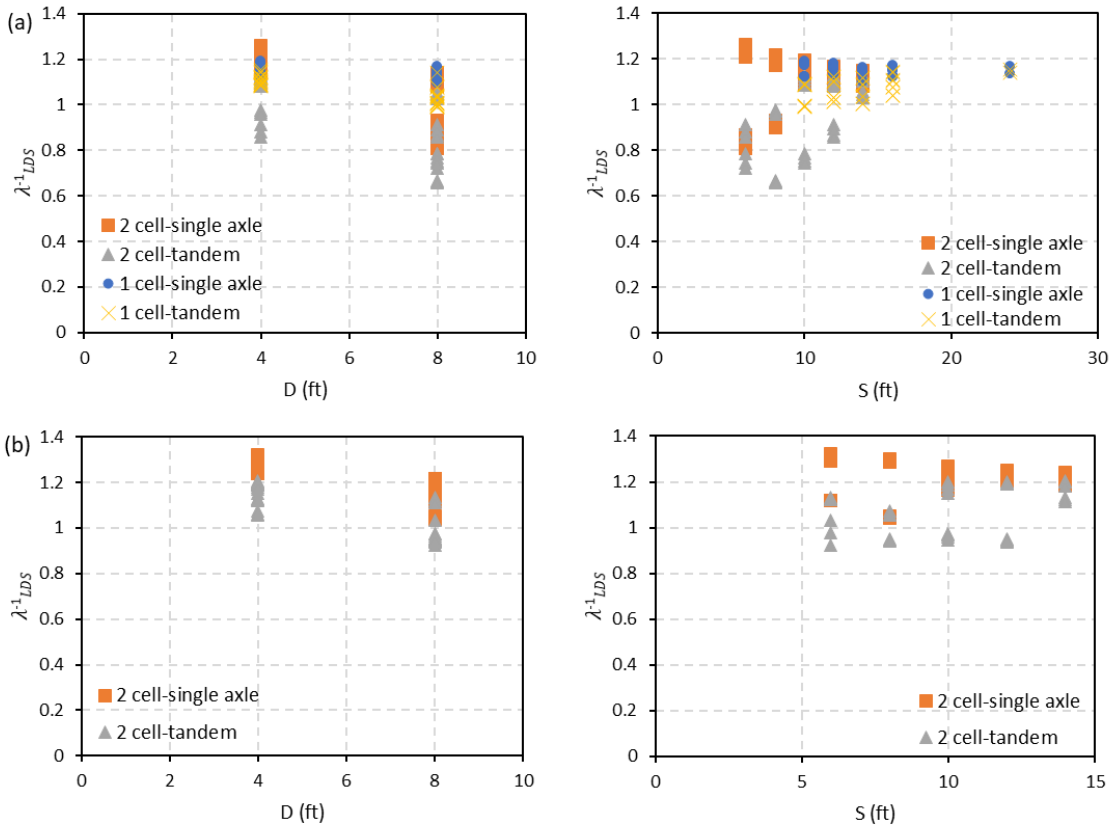

Figure 5.10: Comparison of structural frame model with FE model for shear force at location (a) S1 and (b) S2

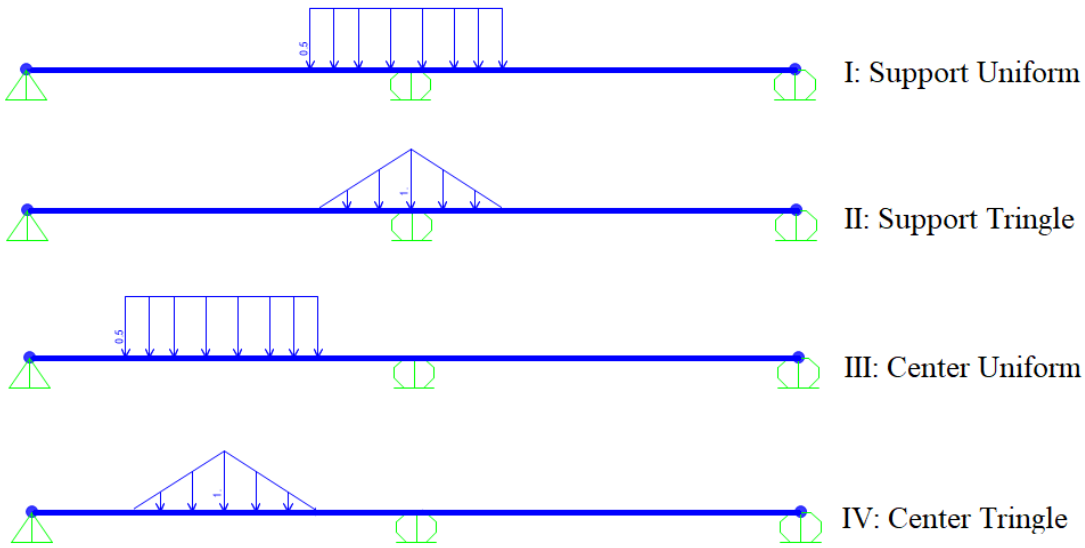

Figure 5.11: Load patterns on the continuous beam

Table 5.3: Comparison of effects due to load pattern

Load case	Midspan positive moment (kip-ft)	Support negative moment (kip-ft)	Moment difference (uniform as baseline)	Support shear (kip)	Shear difference (uniform as baseline)
I: Support uniform	NA	1.2	-28.33%	1.21	1.65%
II: Support triangle	NA	0.86		1.23	
III: Center uniform	3.61	NA	13.30%	NA	NA
IV: Center triangle	4.09	NA		NA	

Note: NA stands these values are not of interest

Chapter 6

Conclusions and Future Work

6.1 Conclusions

The present study focuses on the uncertainty quantification for the live load effects in buried RC box culverts. A comprehensive set of tools and methods has been developed. Firstly, a detailed methodology is developed to estimate the lifetime maxima of live load effects in the buried Reinforced Concrete (RC) box culverts. These live load effect maxima are determined with Monte Carlo simulation considering axle load spectrum involving different axle weights and two types of axle configurations (single and tandem). Gumbel distributions are then derived to model the maximum live load effect over the 75-year design service life. Secondly, a three-dimensional (3D) Finite Element (FE) modeling approach is established for RC box culverts and successfully validated. Using an automated tool developed herein based on OpenSeesPy and Abaqus scripting, the present study systematically investigates the uncertainty in live load distribution (through the backfill) due to the different geometries and properties within the soil-culvert system. From the present study, the following conclusions can be drawn:

- The uncertainty of live load effects in culverts is affected by the axle weight spectrum. However, this uncertainty may be overshadowed by those due to site variability and limited weigh-in-motion data.

- The validation of the developed 3D FE indicates that the selection of reference surface for the shell element representing the culvert affects the bending moment in both slab and walls of a culvert.
- The peak pressure on the top slab of a culvert is lower when the tire is placed near or right above the external wall of a culvert. It increases as the location of the tire approaches the midspan. For two-cell culverts, the peak pressure on the top slab decreases slightly when the tire moves from above the cell midspan to above the interior wall.
- Bending moments at the midspan of a cell and the exterior slab-wall corner are both overestimated in frame analysis compared to FE analysis. For positive bending moment at the midspan, the extent of this overestimation increases as the cell span increases. Similar trend does not occur for the negative bending moment at the corner, although the overestimation is significantly higher for culverts with shorter spans (less than 6 ft). For both load effects, the accuracy of frame analysis does not depend on backfill depths.
- Shear forces at slab-wall corners exhibit more variable and larger discrepancy between estimations from frame and FE analyses. For some culverts, the shear forces estimated by frame analyses are lower than those by FE analysis. The epistemic uncertainty related to frame analysis seems to be related to backfill depths and not sensitive to span lengths, though more studies are needed to confirm this observation.

6.2 Future Works

The findings of this study pave the way for future research to enhance the understanding of live load effects in RC box culverts and improve design equations. Some potential areas for future work include:

- Calibration of projected live load effects and epistemic uncertainty of LRFD live load distribution model under tridem and quad load patterns. This calibration process can enhance the accuracy of the uncertainty model for a broader range of loading conditions.
- Utilize the results obtained in this study to conduct a comprehensive risk and reliability analysis for culvert structures. This analysis can contribute to determining appropriate load factors and target reliability indices for RC box culverts.
- Investigate additional backfill depths other than 4 ft and 8 ft considered in the current analysis. Consideration of a wide range of backfill depths (low backfill included) can offer a more complete understanding of the structural safety of RC box culverts.
- Implementing advanced soil-structure interaction (SSI) models that account for non-linear soil behavior including plasticity. This is especially important when extending the uncertainty quantification approach developed herein to flexible culverts such as corrugated metal culverts.

References

AASHTO, 2002. *LRFD Highway Bridge Design Specifications,* Washington, D.C.: American Association of State Highway and Transportation Officials.

AASHTO, 2018. *The Manual for Bridge Evaluation,* Washington, DC.

AASHTO, 2019. *LRFD bridge design specifications,* Washington, DC.

ABAQUS, 2019. *ABAQUS/Standard User's Manual, Version,* United States: Dassault Systems Simulia Corp.

Acharya, R., Han, J. & Parsons, R., 2016. Numerical analysis of low-fill box culvert under rigid pavement subjected to static traffic loading. *International Journal of Geomechanics,* 16(5), p. 04016016.

ASTM C789-95, 1995. *slandered specification for precast reinforced concrete box section for culvert, storm drains and sewers.*

Han, J., Acharya, R., Parsons, R. L. & Khatri, D., 2009. *Improved load distribution for load rating of low-fill box structures,* Kansas DOT, Topeka, KS: Final Rep. No. K-Tran KU-12-3.

Kadivar, M., Manahiloh, K. N., Kaliakin, V. N. & Shenton, H. W., 2018. *Assessment of dynamic load allowance for buried culverts.* IFCEE 2018 GSP 297.

Katona, M. G., 2019. Improved methods for simulating live loads for two-dimensional structural analysis of buried culverts. *Transportation Research Record,* 2673(12), pp. 449-462.

Lawson, W. D., Seo, H., Surles, J. G. & Morse, S. M., 2018. Impact of specialized hauling vehicles on load rating older, bridge-class, reinforced concrete box culverts. *Transportation Research Record,* 2672(41), pp. 87-100.

Lawson, W. D., Wood, T. A., Newhouse, C. D. & Jayawickrama, P. W., 2010. *Evaluating existing culverts for load capacity allowing for soil structure interaction,* Texas DOT, Austin, TX: FHWA/TX-10/0-5849-1, Texas DOT.

McGrath, T. J., Liepins, A. A. & Beaver, J. L., 2005. Live load distribution widths for reinforced concrete box sections. *Transportation Research Record: Journal of the Transportation Research Board.*

McKenna, F., 2011. OpenSees: A framework for earthquake engineering simulation. *Computing in Science & Engineering,* 13(4), p. 58–66.

NCHRP, 2015. *Proposed modifications to AASHTO culvert load rating specification,* Washington, DC: NCHRP 15-54.

Nowak, A. S., 1999. *Calibration of LRFD bridge design code,* Washingtorç D.C: NCHRP report 368.

Nowak, A. S. & Collins, K. R., 2012. *Reliability of structures.* CRC Press.

O'Brien, E. J. et al., 2005. Procedures for the assessment of highway structures.. *In Proceedings of the Institution of Civil Engineers-Transport,* 158(1), pp. 17-25.

Orton, S., Loehr, J., Boeckmann, A. & Havens, G., 2015. Live-load effect in reinforced concrete box culverts under soil fill. *Journal of Bridge Engineering,* 20(11), p. 04015003..

Petersen, D. L., Nelson, C. R., Li, G. & McGrath, T. J. K. Y., 2010. *Recommended Design Specifications for Live Load Distribution to Buried Structures,* WASHINGTON, D.C: NCHRP Report, 647.

Rund, R. & McGrath, T., 2000. *Comparison of AASHTO Standard and LRFD Code Provisions for Buried Concrete Box Culverts,* West Conshohocken, Pennsylvania: Concrete Pipe for the New Millennium, ASTM STP 1368.

Scanlon, R. F., 2012. *Detailed visual culvert inspection guidelines. ,* Western Australia: Main Roads .

Schall, J. D., 2012. *Hydraulic design of highway culverts,* Federal Highway Administration.

Sharifi, H., Peiris, A. & Harik, I., 2023. Triage method for load rating bridge size two-cell reinforced concrete box culverts for the AASHTO LRFD design load. *Structure and Infrastructure Engineering,* 19(9), pp. 1235-1248.

Sivakumar, B., Ghosn, M. & Moses, F., 2011. *Protocols for collecting and using traffic data in bridge design,* WASHINGTON, D.C.: NCHRP report 683.

TRB Committee AKB70, 2013. *Research needs statement: Design and load rating of buried structures,* Washington, DC: TRB (Transportation Research Board).

Wood, T. et al., 2016. Improved load rating of reinforced-concrete box culverts using depth-calibrated live-load attenuation. *Journal of Bridge Engineering,* 21(12), p. 04016095.

Zhu, M., McKenna, F. & Scott, M., 2018. OpenSeesPy: Python library for the OpenSees finite element framework.. *SoftwareX,* Volume 7, p. 6–11.

Zuo, Z. H. & Xie, Y. M., 2015. A simple and compact Python code for complex 3D topology optimization. *Advances in Engineering Software,* Volume 85, pp. 1-11.

A1: Python script for modeling 3D FE model of RC box culvert

```
from part import *
from material import *
from section import *
from assembly import *
from step import *
from interaction import *
from load import *
from mesh import *
from optimization import *
from job import *
from sketch import *
from visualization import *
from connectorBehavior import *
#### Input Paramters
sheet_size = 200.0 # size of the sheet in for the abaqus grid
ssx = 30.0 # size of soil domain in x-direction(parallel to the traffic)
ssy = 30.0 # size of soil domain in vertical direction
et_d = 18 # szie of soil domain prependicular to the traffic
d_f = 4.0 # back-fill depth
slab_thikness = 12.0/12.0 # slab thickness
wall_thikness = 12.0/12.0 # wall thikeness
span_l = 14.0 # clear span length
wall_h = 12.0 # clear wall height
array_lc = [0.155,  6.045,  15.810, 10.850, 1.705,  4.030,  17.670, 17.515, 2.945]
for lcl in array_lc:
    lc2 = lcl*10000
    # various dimension of plane in soil and culvert
    dt1 = 29.0
    dt2 = 24.0
    dt3 = 19.0
    dt4 = 12.0
    dt5a = -(span_l+wall_thikness-0.83334/2-4/2-9.4333/2.0-lcl)
    dt5b = dt5a-0.83334
    dt5c = dt5a-4.0
    dt5d = dt5b-4.0
    dt5e = 0.0
    dt8 = (span_l)+wall_thikness*3/2
    dt9 = ssy-d_f
    dt10 = ssy-d_f-2*slab_thikness-wall_h
    dt6 = et_d-2.1667
    dt7 = et_d-3.8334
```

```
# creating the soil and hollow box (culvert size) in the soil
mdb.models['Model-1'].ConstrainedSketch(name='__profile__', sheetSize=sheet_size)
mdb.models['Model-1'].sketches['__profile__'].rectangle(point1=(-ssx, ssy), point2=(ssx, 0.0))
mdb.models['Model-1'].sketches['__profile__'].rectangle(point1=(-dt8, dt9), point2=(dt8, dt10))
mdb.models['Model-1'].Part(dimensionality=THREE_D, name='soil', type=DEFORMABLE_BODY)
mdb.models['Model-1'].parts['soil'].BaseSolidExtrude(depth=et_d, sketch=mdb.models['Model-1'].sketch
del mdb.models['Model-1'].sketches['__profile__']
# datum palne in soil
mdb.models['Model-1'].parts['soil'].DatumPlaneByPrincipalPlane(offset=dt1, principalPlane=XZPLANE)
mdb.models['Model-1'].parts['soil'].DatumPlaneByPrincipalPlane(offset=dt2, principalPlane=XZPLANE)
mdb.models['Model-1'].parts['soil'].DatumPlaneByPrincipalPlane(offset=dt3, principalPlane=XZPLANE)
mdb.models['Model-1'].parts['soil'].DatumPlaneByPrincipalPlane(offset=dt4, principalPlane=XZPLANE)
mdb.models['Model-1'].parts['soil'].DatumPlaneByPrincipalPlane(offset=dt5a, principalPlane=YZPLANE)
mdb.models['Model-1'].parts['soil'].DatumPlaneByPrincipalPlane(offset=dt5b, principalPlane=YZPLANE)
mdb.models['Model-1'].parts['soil'].DatumPlaneByPrincipalPlane(offset=dt5c, principalPlane=YZPLANE)
mdb.models['Model-1'].parts['soil'].DatumPlaneByPrincipalPlane(offset=dt5d, principalPlane=YZPLANE)
mdb.models['Model-1'].parts['soil'].DatumPlaneByPrincipalPlane(offset=dt5e, principalPlane=YZPLANE)
mdb.models['Model-1'].parts['soil'].DatumPlaneByPrincipalPlane(offset=dt6, principalPlane=XYPLANE)
mdb.models['Model-1'].parts['soil'].DatumPlaneByPrincipalPlane(offset=dt7, principalPlane=XYPLANE)
mdb.models['Model-1'].parts['soil'].DatumPlaneByPrincipalPlane(offset=dt8, principalPlane=YZPLANE)
mdb.models['Model-1'].parts['soil'].DatumPlaneByPrincipalPlane(offset=-dt8, principalPlane=YZPLANE)
mdb.models['Model-1'].parts['soil'].DatumPlaneByPrincipalPlane(offset=dt9, principalPlane=XZPLANE)
mdb.models['Model-1'].parts['soil'].DatumPlaneByPrincipalPlane(offset=dt10, principalPlane=XZPLANE)
```

```
# creating material for culvert and soil
mdb.models['Model-1'].Material(name='culvert')
mdb.models['Model-1'].materials['culvert'].Density(table=((4.66214, ), ))
mdb.models['Model-1'].materials['culvert'].Elastic(table=((580320000.0, 0.0), ))
mdb.models['Model-1'].Material(name='l1')
mdb.models['Model-1'].materials['l1'].Density(table=((3.7296, ), ))
mdb.models['Model-1'].materials['l1'].Elastic(table=((187200.0, 0.26), ))
mdb.models['Model-1'].Material(name='l2')
mdb.models['Model-1'].materials['l2'].Density(table=((3.7296, ), ))
mdb.models['Model-1'].materials['l2'].Elastic(table=((302400.0, 0.21), ))
mdb.models['Model-1'].Material(name='l3')
mdb.models['Model-1'].materials['l3'].Density(table=((3.7296, ), ))
mdb.models['Model-1'].materials['l3'].Elastic(table=((374400.0, 0.19), ))
mdb.models['Model-1'].Material(name='l4')
mdb.models['Model-1'].materials['l4'].Density(table=((3.7296, ), ))
mdb.models['Model-1'].materials['l4'].Elastic(table=((475200.0, 0.19), ))
mdb.models['Model-1'].Material(name='l5')
mdb.models['Model-1'].materials['l5'].Density(table=((3.7296, ), ))
mdb.models['Model-1'].materials['l5'].Elastic(table=((475200.0, 0.19), ))
```

```
# select the element where the response need to be calculated
mdb.models['Model-1'].rootAssembly.Set(elements=mdb.models['Model-1'].rootAssembly.instances['culvrt-1'].elements.
    getByBoundingBox(xMin=-dt8, yMin=dt9, zMin=-1.5, xMax=-dt8+0.75, yMax=dt9, zMax=-0.4), name='left corner sl')
mdb.models['Model-1'].rootAssembly.Set(elements=mdb.models['Model-1'].rootAssembly.instances['culvrt-1'].elements.
    getByBoundingBox(xMin=-0.8, yMin=dt9, zMin=-1.5, xMax=0, yMax=dt9, zMax=-0.4), name='right corner sl')
mdb.models['Model-1'].rootAssembly.Set(elements=mdb.models['Model-1'].rootAssembly.instances['culvrt-1'].elements.
    getByBoundingBox(xMin=0, yMin=dt9, zMin=-1.5, xMax=0.8, yMax=dt9, zMax=-0.4), name='left corner s2')
mdb.models['Model-1'].rootAssembly.Set(elements=mdb.models['Model-1'].rootAssembly.instances['culvrt-1'].elements.
    getByBoundingBox(xMin=-dt8/2-0.6, yMin=dt9, zMin=-1.5, xMax=-dt8/2+0.6, yMax=dt9, zMax=-0.4), name='mid span sl')
mdb.models['Model-1'].rootAssembly.Set(elements=mdb.models['Model-1'].rootAssembly.instances['culvrt-1'].elements.
    getByBoundingBox(xMin=-dt8, yMin=dt9-0.5, zMin=-1.5, xMax=-dt8, yMax=dt9, zMax=-0.4), name='left wall')
mdb.models['Model-1'].rootAssembly.Set(elements=mdb.models['Model-1'].rootAssembly.instances['culvrt-1'].elements.
    getByBoundingBox(xMin=0, yMin=dt9-0.5, zMin=-1.5, xMax=0, yMax=dt9, zMax=-0.4), name='mid wall')
```

```
# apply the load on the culvert on the selected surface
mdb.models['Model-1'].Pressure(amplitude='Amp-1', createStepName='Step-1', distributionType=UNIFORM, field='',
    magnitude=360.0, name='Load-1', region=mdb.models['Model-1'].rootAssembly.surfaces['loadsurf'])
mdb.models['Model-1'].Pressure(amplitude='Amp-1', createStepName='Step-1', distributionType=UNIFORM, field='',
    magnitude=360.0, name='Load-2', region=mdb.models['Model-1'].rootAssembly.surfaces['loadsurf-1'])
# apply the boundary condition on the selected node
mdb.models['Model-1'].ZsymmBC(createStepName='Step-1', localCsys=None, name='BC-2',
    region=mdb.models['Model-1'].rootAssembly.sets['z-node'])
mdb.models['Model-1'].DisplacementBC(amplitude=UNSET, createStepName='Step-1', distributionType=UNIFORM,
    fieldName='', fixed=OFF, localCsys=None, name='BC-3', region=mdb.models['Model-1'].rootAssembly.sets['base'],
    u1=0.0, u2=0.0, u3=0.0, ur1=UNSET, ur2=UNSET, ur3=UNSET)
mdb.models['Model-1'].DisplacementBC(amplitude=UNSET, createStepName='Step-1', distributionType=UNIFORM,
    fieldName='', fixed=OFF, localCsys=None, name='BC-4', region=mdb.models['Model-1'].rootAssembly.sets['side'],
    u1=0.0, u2=UNSET, u3=0.0, ur1=UNSET, ur2=UNSET, ur3=UNSET)
# create the job
mdb.Job(atTime=None, contactPrint=OFF, description='', echoPrint=OFF, explicitPrecision=SINGLE,
    getMemoryFromAnalysis=True, historyPrint=OFF, memory=90, memoryUnits=PERCENTAGE, model='Model-1', modelPrint=OFF,
    multiprocessingMode=DEFAULT, name='Job-' + str(int(lc2)), nodalOutputPrecision=SINGLE, numCpus=4,
    numDomains=4, numGPUs=0, queue=None, resultsFormat=ODB, scratch='',
    type=ANALYSIS, userSubroutine='', waitHours=0, waitMinutes=0)
# submit the job
mdb.jobs['Job-' + str(int(lc2))].submit(consistencyChecking=OFF)
```